Protons Associated With Centers of Solar Activity and Their Propagation in Interplanetary Magnetic Field Regions Co-rotating with the Sun*

C. Y. Fan† and M. Pick‡
Enrico Fermi Institute for Nuclear Studies

and

R. Pyle§, J. A. Simpson and D. R. Smith§
Enrico Fermi Institute for Nuclear Studies and
Department of Physics
University of Chicago
Chicago, Illinois 60637

Laboratory for Astrophysics and Space Research

EFINS Preprint No. 67-72

August 1967

* This research was supported in part by the National Aeronautics and Space Administration under grant NsG 179-61, and NAS 2-3876, and the U. S. Air Force Office of Scientific Research under Contract AF 39 (638)1642.

† Now at Department of Physics, University of Arizona.

‡ On leave from Meudon Observatory, Meudon, France.

§ NASA predoctoral trainee.

Protons Associated With Centers of Solar Activity and Their Propagation in Interplanetary Magnetic Field Regions Co-rotating with the Sun*

C. Y. Fan† and M. Pick‡
Enrico Fermi Institute for Nuclear Studies
and
R. Pyle§, J. A. Simpson and D. R. Smith§
Enrico Fermi Institute for Nuclear Studies and
Department of Physics
University of Chicago
Chicago, Illinois 60637

ABSTRACT

The Pioneer-6 and Pioneer-7 space probes carried charged-particle telescopes which measure, for the first time, both the direction of arrival and differential energy spectra of protons and alpha particles. The intensity changes, directional distributions and energy spectra of proton fluxes associated with solar activity are investigated. The data were obtained in the beginning of the new solar cycle (No. 20), when it is possible to unambiguously associate proton flux increases with specific solar active regions. The origin, possible long-term storage, and propagation of these proton fluxes are investigated. It was observed that enhanced 0.6 - 13 MeV proton fluxes associated with specific active regions were present over heliographic longitude ranges as great as ~ 180 degrees. These enhanced fluxes exhibit definite onsets and cut-offs which appear to be associated with the magnetic sector boundaries observed by Ness on Pioneer-6. Discrete flare-produced

---

* This research was supported in part by the National Aeronautics and Space Administration under grant NsG 179-61, and NAS 2-3876, and the U. S. Air Force Office of Scientific Research under Contract AF 39 (638) 1642.

† Now at Department of Physics, University of Arizona.

‡ On leave from Meudon Observatory, Meudon, France.

§ NASA predoctoral trainee.

intensity increases extending in energy to more than 50 MeV are observed, superposed on the enhanced flux. These increases displayed short transit times and short rise times. Both the enhanced and flare-produced fluxes propagate along the spiral interplanetary magnetic field from the western hemisphere of the Sun. From these observations we are led to a model in which the magnetic fields from the active center are spread out over a longitude range of 100 - 180 degrees in the solar corona. The existence of strong unidirectional anisotropies in the initial phases of flare proton events implies that little scattering occurs between the Sun and spacecraft. However, the gradual approach to an isotropic flux at late times indicates that the decay phase is controlled by the interplanetary magnetic field.

I. INTRODUCTION

Satellite studies of interplanetary proton fluxes in the energy range 1 - 20 MeV have shown that there is an approximate 27-day recurrence of enhanced flux confined to sector-like structures in the interplanetary magnetic fields which co-rotate with the Sun (Bryant et al., 1965; Fan, Gloeckler and Simpson, 1964, 1966; Ness and Wilcox, 1965). These recurring proton fluxes were present continuously for about 10 days, indicating that the magnetic field structure within which the protons propagated extended in heliocentric longitude over more than 100 degrees. Since these observations were made near solar minimum (1963 - 1965) no identification with solar active regions was possible (Fan, Gloeckler and Simpson, 1966) and therefore, although these protons appeared generally to be of solar-system origin, it could not be decided whether they were accelerated in processes like solar flares or whether they were undergoing continual acceleration in the interplanetary medium.

More recently, with the development of the new solar cycle, low-energy proton flux increases from identified flares were observed over a longitudinal range in space similar to that found earlier for the recurring proton fluxes. Simultaneous observations were made by the Mariner-4 and IMP-3 spacecraft at widely separated heliographic longitudes during 1965. Some of these flux increases were shown (O'Gallagher and Simpson, 1966) to be confined to co-rotating magnetic field regions.

The Pioneer-6 and Pioneer-7 space probes were launched in December 1965 and August 1966 respectively, carrying instruments which made it possible for the first time to measure both the direction of arrival and differential energy spectra of protons and alpha particles and to distinguish them from electrons. It was found that, on the average, solar-flare proton fluxes of ~ 10 MeV displayed large anisotropies directed primarily along the prevailing spiral angle of the interplanetary magnetic field (Fan,

Lamport, Simpson and Smith, 1966; McCracken and Ness, 1966). This very high degree of anisotropy is explained by propagation of the particles with low pitch angles along the direction of the magnetic lines of force.

All of the above studies raise questions as to 1) whether there is more than one origin for the low-energy protons (e.g. acceleration in solar active centers or in interplanetary space); 2) whether there is a long-term storage of flare-accelerated protons in the magnetic fields close to the Sun; and 3) the way in which the source of the low-energy protons is connected with the interplanetary magnetic field lines along which these protons are confined to propagate.

In this paper we present the results of measurements which bear on these questions. The data were obtained with the University of Chicago charged-particle telescopes on Pioneer-6 and Pioneer-7 during the period December 1965 to September 1966.

With increased solar activity and the appearance of strong centers of activity, we find:

A. The heliographic longitudinal range over which enhanced proton fluxes > 0.6 MeV are continuously observed in interplanetary space may be as great as ~ 180 degrees.

B. This flux of low-energy protons is observed to exhibit definite onsets and cut-offs.

C. The interplanetary regions within which these low-energy protons are confined are also observed to modulate the galactic cosmic radiation.

D. Superposed on the 0.6 MeV flux level are occasional large and

discrete flare-produced intensity increases extending in energy to more than 50 MeV for protons.

E. These proton fluxes are associated with specific active regions on the Sun within which the principal flare activity resides.

F. The protons from discrete solar flares propagate along magnetic lines of force in interplanetary space which connect with the active solar centers.

From these observations we are led to a quasi-stationary model for the distribution of magnetic fields above the active center in which the fields are spread out in the corona over a range of $\sim 180^{\circ}$ longitude (possibly due to the presence of superheated coronal plasma), and then extended into interplanetary space.

II. DESCRIPTION OF SPACECRAFT AND INSTRUMENT

Pioneer-6 and Pioneer-7 are spin-stabilized deep-space probes which were launched into heliocentric orbits on 16 December 1965 and 17 August 1966, respectively. Pioneer-6 was launched inward from Earth in an orbit with a perihelion of 0.815 A.U. and a period of 311 days, and Pioneer-7 was launched outward into an orbit with an aphelion of 1.125 A.U. and a period of 403 days. Each spacecraft is oriented with its spin axis pointing towards the south ecliptic pole so that the University of Chicago charged-particle telescope (Figure 1), mounted with its major axis perpendicular to the spacecraft spin axis, makes a 360° scan in the ecliptic plane approximately once each second. The data used for analysis in this paper were collected when the two spacecraft were in the vicinity of the Sun-Earth line ($< 4.0 \times 10^{7}$ km from Earth and < 0.18 A.U. from the orbit of Earth), but well outside the influence of the magnetosphere. The initial portion of the Pioneer-6 trajectory is shown in Figure 1 of Fan, Lamport,

Simpson and Smith (1966).

A schematic drawing of the charged-particle telescope on the two space probes is shown in Figure 1. It consists of three stabilized, lithium-drifted silicon detectors D_1, D_2 and D_3, separated by two absorbers A_2 and A_3. A_1 is an aluminized mylar window to exclude solar illumination on D_1. It is especially important to note the cylindrical plastic scintillator D_4 viewed by a photomultiplier tube which is in anticoincidence with the three silicon detectors to protect against background events. This arrangement is essential for the measurement of particle fluxes as low as $\sim 10^{-3}$ particles/cm^2 sec ster. The particle range intervals determined by coincidence combinations of the detectors are summarized in Table 1. For each range interval shown, the counting rate was transmitted by the spacecraft telemetry. The counting rate of the D_4 anticoincidence detector was also monitored.

A functional test of the detectors was made in a special mode of operation (calibrate mode) upon command from Earth. In this mode the individual detector counting rates were measured. No radioactive calibration sources which might prevent the detection of small flux levels were employed.

We obtain particle identification (e.g. proton, helium nucleus, electron, etc.) by the simultaneous measurement of energy loss and range. The energy loss in D_1 was measured by a 128-channel pulse-height analyzer for particles which fulfill the range condition $D_1 D_2 \bar{D}_4$. In addition, the energy loss in D_3 was measured by a 32-channel analyzer if the particle penetrated to D_3. Thus, the differential energy spectra for protons and helium nuclei may be uniquely determined in the energy range 13 to 100 MeV/nucleon. The Pioneer-7 instrument was modified to permit the additional pulse-height analysis of $D_1 \bar{D}_4$ events in calibrate mode, controlled by commands

from Earth. In this mode of operation the measurements of differential spectra could be extended downwards to the energy range 0.6 to 13 MeV/nucleon.

The direction of arrival of each analyzed particle was determined by dividing the complete scan of 360° in the ecliptic plane into eight overlapping sectors of 45° nominal width. For each rotation of the spacecraft a sun-sensor on the spacecraft provided a signal which initiated a sequential count of sector number. For each particle event that was pulse-height analyzed the sector number at the time of detection was telemetered, together with the pulse-height channel. The spin rate was measured throughout the mission so that in the analysis of the data, the sectors could be weighted to yield equal "exposure" times in order to avoid a bias in the directional distributions. A second system for determining directional distributions counted in quadrants all particles which fulfilled the range condition $D_1 D_2 \bar{D}_3 \bar{D}_4$. A discussion of our analysis of the directional information from these two systems appears in Appendix II.

During the period within which the data were recorded on the Pioneer spacecraft, the IMP-3 satellite experiment of the University of Chicago carried out similar measurements in interplanetary space near Earth (apogee ~ 30 Earth radii). For the present investigation we have used simultaneous observations by the IMP-3 charged-particle telescope, which has been described by Fan, Gloeckler, Hsieh and Simpson (1966).

III. EXPERIMENTAL RESULTS

Since protons are the major charged-particle component observed in fluxes of solar origin, we shall confine our attention to the analysis of proton data, and investigate the intensity changes, directional distributions, and differential energy

spectra of fluxes associated with solar activity. In Figure 2 we display, by solar rotations, one-hour averages of the $D_1 D_2 \bar{D}_3 \bar{D}_4$ coincidence counting rate (13-70 MeV protons) for the time periods 24 December 1965 through 7 May 1966 from Pioneer-6, and 24 August through 19 September 1966 from Pioneer-7. A well-defined "background" counting rate is observed which is due primarily to the galactic flux of protons and helium nuclei in the energy range 13-70 MeV/nucleon. This background counting rate undergoes a slow, steady decrease due to modulation of the galactic flux as the new solar cycle begins. Superposed on this steady background are well-defined increases in counting rate which are due to solar flare protons. The period 14-31 March is analyzed in detail in the following sections.

In Figures 3, 4 and 5 we show the $D_1 \bar{D}_2 \bar{D}_4$ counting rate (protons 0.6-13 MeV) for selected time intervals. For this counting rate, a well-defined background level also exists. This background level of $\sim$ 0.1 counts per second is due primarily to the "quiet-time" proton flux reported by Fan et.al.(1968) to be present in the period 1964-1966 with a steeply-falling differential energy spectrum. We have found (in section V) that the differential energy spectrum of protons observed by Pioneer-7 at quiet times has the form $E^{-2.8}$ in the energy interval 0.8 to 6 MeV. Thus, the mean energy of the background proton flux is $E \sim 1$ MeV for the 0.6-13 MeV counting-rate channel ($D_1 \bar{D}_2 \bar{D}_4$). As we pointed out in section II, the protection of D_1 by an anticoincidence detector is essential for the observation of the extremely low proton flux levels we have observed in interplanetary space. We emphasize that a single D_1 detector without anticoincidence shielding (e.g., O'Gallagher and Simpson, 1966) or a detector with small geometrical factor and alpha-source calibration (e.g., Krimigis and Van Allen, 1966) has poor statistics and background which would conceal the

presence of some of the phenomena we report in this paper. That is, the Pioneer instruments are capable of detecting flux changes as small as $\sim 10^{-3}$ particles/cm^2 sec ster with time resolution of $\sim$ 1 hr.

A comparison of Figures 3, 4 and 5 with the corresponding time intervals in Figure 2 indicates that, in general, the increase of particle flux above the background at lower energies is of greater duration than at higher energies (see Table 2). At some time prior to the occurrence of a solar-flare effect in the higher energy interval, the low-energy flux begins a more or less steady increase above the prevailing background. We define the start of this increase as the "proton flux onset." In Figure 6 we have displayed, on an expanded scale, some of the proton flux onsets which we consider in detail in following sections. At later times discrete flare effects are visible at low energies (0.6 - 13 MeV) with corresponding increases above background at higher energies (13 - 70 MeV). After reaching a maximum value, the low-energy counting rate begins to decrease, although "structure" frequently appears in the counting-rate curve. Finally the counting rate either drops sharply to background (e.g., 4 January 1966) or runs smoothly into the background (e.g., 10 April 1966). We define this point as the "proton flux cut-off."

The data in Figures 2, 3, 4 and 5 are proton intensity "profiles" which are composed of both strongly time-dependent events, i.e. solar flares, and quasi-steady-state flux distributions confined within the magnetic field co-rotating with the Sun (O'Gallagher and Simpson, 1966; Fan, Gloeckler and Simpson, 1966). It is important to keep in mind these distinctions of temporal and spatial flux distributions in the discussions which follow in this paper. There are many time intervals where we have observed a co-rotation effect (Fan, Lamport, Simpson and Smith, 1966) of an outstanding

feature on the counting-rate curve by simultaneous measurements of proton flux on the Earth satellite IMP-3 and the Pioneer-6 or Pioneer-7 space probes. These time intervals are indicated in Figures 3 and 5.

To indicate the presence of large-scale interplanetary magnetic structures we have made use of the well-established fact that such structures modulate the cosmic-ray flux from the galaxy (e.g. 27-day recurring intensity decreases or flare-produced shock waves, Meyer and Simpson, 1954; McCracken, Rao and Bukata, 1966). For this purpose we have included the neutron monitor intensity modulation for cosmic rays > 3000 MV magnetic rigidity in Figures 3, 4 and 5 from the Climax neutron monitor.

IV. IDENTIFICATION OF SOLAR ACTIVE CENTERS ASSOCIATED WITH PROTON FLUX INCREASES

During this period of the present solar cycle we are fortunate to be able to unambiguously associate proton flux increases with specific regions on the visible solar disk. It is the purpose of this section to outline the methods of identification using both optical and radio data. The period covered by our study extends from December 1965 through April 1966 using the Pioneer-6 data in the period of nearly continuous telemetry coverage. We have also used data from IMP-3 in July 1966, and the first month of the Pioneer-7 mission, from August into September 1966.

We have examined centers of solar activity present on the visible solar disk during the period of enhanced low-energy flux. The identification of the responsible center is based chiefly upon its optical and radio characteristics (the slowly-varying component) and on its yield of 10-cm radio bursts. All optical flares do not give radio bursts (Kundu, 1959); however, energetic high-frequency radio bursts are more indicative of a particle-producing flare than optical importance. The presence of outstanding 10-cm

radio bursts is a particularly good indicator of flares which produce high-energy protons (Avignon and Pick, 1959; Hakura and Goh, 1961; Kundu and Haddock, 1960; Caroubalos, 1964). A description of the nine selected centers is given in Table 3. We emphasize that this list is not complete; it does not indicate all the centers of activity but only a selection of the important ones as defined by criteria which we discuss below.

For each center we give the identification numbers of the McMath Observatory and the Quarterly Bulletin on Solar Activity, the Carrington coordinates (reference axes fixed on the solar surface), and the day of central meridian passage of the center. For each center considered we have included also the other centers of activity present on the solar disk which could have led to difficulty in making a unique identification. The total number of optical flares and of 10-cm radio bursts are also given in Table 3. Class 1^- flares are not included unless they are associated with 10-cm radio bursts. The number of 10-cm radio bursts is a lower limit since the available observations do not cover the entire day. The last two columns give the number of 10-cm radio bursts clearly associated with the identified center and the total number for the period during which the center was on the visible solar disk. For the majority of cases we see that the number of optical flares associated with the chosen center is very great compared with all other centers of activity on the disk at that time. A comparison of the numbers of radio bursts shows even more dramatically the predominance of one center.

In Table 4 the selected solar regions are listed in the first column and a brief history of the center is given in column 2. In the last two columns we give the dates and the solar longitude of the active center for the onset and cut-off of the proton fluxes. The solar longitude is referred to central meridian as viewed from the

spacecraft. The data in Table 4 are summarized in Figure 7, which shows the longitudinal range of solar active centers over the time intervals for which we observe enhanced low-energy proton fluxes. In addition, discrete flare-produced increases in the 13-70 MeV proton flux are indicated in the figure.

Of all the centers chosen there exist two cases (8413-8414; 8459-8461) for which it is possible that another region present at the same time may be responsible for the onset of the proton fluxes, and three cases (8240, 8262, 8362) where the same confusion may exist at the cut-off of the proton flux.

We consider three special cases:

A. Centers of solar activity appearing at the east limb. An example is region 8131. The enhanced proton flux that was attributed to this region is shown in Figure 3. The onset of 0.6 MeV protons on 13 January occurs when the active region reaches a longitude of 75° East. The low-energy proton flux then increases until the occurrence of the first large flares associated with important radio bursts and higher-energy protons. There are many small flares in this region until 17 January when the proton flux level in both the 0.6-13 and 13-70 MeV ranges increases rapidly. On this day a class 2 flare occurred at 1032 U.T., associated with a type IV radio burst. At later times, the counting rate decreases until 28 January when there is a proton flux cut-off. At that time the solar active center is ~ 130° West.

B. Centers of activity born or developing on the visible disk. Examples are regions 8105, 8240, and 8362 (see Table 4). In these cases the

proton fluxes appear within a few days after the birth or development of the region. They persist until the proton flux cut-off when the active center is ~ 130° West, as for case A above.

C. Centers of activity followed by a second center. Examples are the regions 8207, 8223 and 8240 which are followed by regions 8223, 8240, and 8262, respectively. In Figure 4 we note a particularly striking sequence of events wherein the solar region 8207 is associated with the enhanced 0.6 - 13 MeV proton flux from 15 - 31 March. It is followed by a second important region (8223) associated with a similar intensity-time profile which is of smaller amplitude. These solar regions are identified in Figure 8 which represents the synoptic map of the chromosphere from Meudon Observatory. Although region 8223 produced many radio bursts and large optical flares after its appearance on the east limb on 27 March there is no evidence that we observe protons from this region until 31 March. At this time region 8207 reached a solar longitude of ~ 130° W. It is interesting to note that an interplanetary magnetic field sector boundary passed the spacecraft on this day (Ness, 1967). It is possible, however, that the enhanced low-energy proton flux during the period 27 - 31 March may be made up of contributions from both these centers. There were no discrete 13 - 70 MeV proton events associated with region 8223.

V. THE SOLAR ORIGIN AND PROPAGATION OF THE PROTON FLUX

The association of solar active centers with enhanced proton fluxes at low energies, as summarized in Figure 7, is strong evidence for the solar origin of these

protons. We now present experimental evidence to prove their solar origin by showing that they propagate from the solar corona along the interplanetary magnetic field and that their energy spectrum is similar to solar flare proton spectra.

A. Spectrum and directional distribution of the 0.6 - 13 MeV proton flux during "quiet times."

We first investigated the characteristics of the quiet-time flux which was observed as a steady background for several days in each solar rotation period. The level of this flux measured by the Pioneer-6 and Pioneer-7 instruments is approximately constant over the 9-month period discussed in this paper.

The directional distribution and differential energy spectra of the 0.6 to 13 MeV proton fluxes could not be examined until after 17 August at which time Pioneer-7 was launched with its additional low-energy mode of analysis (Table 1, Section II). On 20-21 August 1966 (Figure 5) we measured the differential energy spectrum shown as the dashed line (a) in Figure 9. This quiet-time proton spectrum is the same as the spectrum for the 1 to 20 MeV proton fluxes measured at approximately the same time on OGO-3 (Fan et al., 1968). Although it has been shown by Fan et al. (1968) that this quiet-time proton flux is not instrumental in origin, we do not know at present what fraction of the flux is solar and what fraction is galactic.

We have examined the directional distribution of this quiet-time flux of protons, as shown in Figure 10 (a). Using the method of analysis discussed in Appendix II, the observed anisotropy is $< 8\%$.

B. Directional distribution and energy spectrum of enhanced 0.6 - 13 MeV proton flux.

We have found in Sections III and IV that low-energy protons associated

with a solar active center are observed at the spacecraft for periods of a few days before the appearance of higher-energy flux increases associated with discrete flares. The most outstanding examples of these periods are the following:

a. 25 - 26 December 1965 (Figure 3)

b. 13 - 17 January 1966 (Figure 3)

c. 15 - 20 March 1966 (Figure 4)

d. 3 - 7 July 1966 (Figure 6)

e. 22 - 28 August 1966 (Figure 5).

Within these time periods the flux of 0.6 - 13 MeV protons generally increases at least 20 percent above the quiet-time flux. Additional examples of these proton flux onsets are listed in Table 4.

Beginning with the proton flux onset on 22 August (Figures 5 and 6) we examined the energy spectrum and the directional distribution over the period ending with the commencement of the large solar flare event of 28 August. The differential energy spectra at these times are shown in Figure 9. The analysis was cut off below 0.8 MeV to eliminate any possible solar electron flux contribution. The steep negative slopes in curves (b) and (c) explain why investigators using instruments with higher energy thresholds (e.g. McCracken, Rao and Bukata, 1966) do not observe the extensive periods of low-energy flux enhancements which we report here.

We show in Figure 10(b) and (c) the directional distributions of the enhanced flux; they are typical of the entire period. We have removed the quiet-time background distribution shown in Figure 10(a) to obtain these distributions. The prevailing arrival direction of the particle flux at 1 A.U. is approximately 30° to 40° West of the Sun-spacecraft line. These measurements are conclusive evidence that the en-

hanced 0.6 - 13 MeV proton flux was propagating from the Sun along the direction of the interplanetary magnetic field which on the average departs from the corona ~ 50° west of central meridian.

We assume that the directional distributions and energy spectra deduced from Pioneer-7 for both "quiet-time" and enhanced fluxes apply to the observations for Pioneer-6 because (a) the 0.6 - 13 MeV proton flux enhancements measured by Pioneer-7 have intensity-time profiles and related solar characteristics similar to the flux enhancements we have measured with Pioneer-6 (Figures 3 and 4), and (b) the OGO-3 proton-alpha particle telescope recorded similar background flux levels and proton differential energy spectra in the period December 1965 - August 1966 (Fan et al., 1968). This assumption is implicit in the discussions which follow.

C. Identification of interplanetary magnetic field regions by enhanced proton fluxes.

From the relative positions of the solar active centers with respect to the enhanced proton fluxes as shown in Figure 7, we may now determine the longitudinal distribution of these fluxes close to the Sun from well-established properties of the interplanetary magnetic field. First, it is clear from the analysis of ~ 10 MeV proton propagation (McCracken and Ness, 1966; Fan, Lamport, Simpson, and Smith, 1966) that 1 MeV protons must also propagate along the direction of the magnetic lines of force. Thus, it is possible to use the 1 MeV protons as tracers for delineating the distribution and structure of magnetic fields to which the solar protons have access near the Sun. Second, in interplanetary space the magnetic lines of force take the shape of an archimedes spiral as determined by the average characteristics of the solar wind (Parker, 1963).

Hence, from the observed directional distributions, we know that protons must be coming from a region in the upper corona approximately 50° west of central meridian. It then follows that enhanced proton fluxes associated with the solar active centers are continuously leaving the upper corona at this longitude, from the time of proton flux onset when the center is $\sim 70^{\circ}$ East until the proton flux cut-off when the center is $\sim 130^{\circ}$ West. Therefore, the interplanetary magnetic field region within which the protons propagate extends over a longitudinal range of $\sim 180^{\circ}$. This is equivalent to proton emission from the upper corona over this longitudinal range. We have illustrated these conclusions by a sketch in Figure 11 of the interplanetary magnetic field lines extending outward from the solar corona. The dashed circle in the upper corona represents the elevation at which co-rotation of the magnetic field lines establishes their spiral form. Thus we see that the onsets and cut-offs of proton fluxes (Table 4) correspond to the entry into and exit from interplanetary magnetic field regions co-rotating with the Sun.

If the enhanced fluxes of 0.6-13 MeV protons have their origin in the active centers, the basic question arises as to how they propagate in the corona to the interplanetary magnetic field lines over this wide range of longitudes. Are there lines of force extending from the active center to the upper corona (dashed line in Figure 11) over the required longitudinal range, or is diffusion in the coronal magnetic fields the principal mechanism? To answer these questions we must turn to experimental observations of discrete solar flare events, which provide information on the propagation characteristics of flare protons.

D. Propagation of protons from identified solar flares.

We know in general that there are many competing effects which make difficult the identification of the dominant mode of proton propagation within the

solar corona. Therefore it is most important to search for the least complicated conditions in order to investigate various models. The time interval 13 March - 11 April, 1966 (Figure 4) is an unusually revealing and definitive period for study (Simpson, 1966) which appears simple to interpret relative to other periods.

Solar region 8207 (Figure 7) appeared on the solar disk on 15 March and produced almost all the solar flares observed for many days (Table 3). When this region reached approximately 80° East the 0.6 - 13 MeV proton flux onset was observed at the spacecraft. During the passage of the center to ~ 50° West the 0.6 MeV proton flux had increased above the quiet-time level by a factor of $\sim 5 \times 10^3$, as shown in Figure 4. After the center reached ~ 30° East (19 March) large flares began to produce recognizable proton intensity increases extending in energy above 13 MeV. These solar proton events are identified in Figure 4 as (a), (b), (c), (e), (f) and (h) for the proton fluxes in the energy range 13 - 70 MeV. For each of these events, except (h), there is a corresponding increase above the ambient flux level in the 0.6 - 13 MeV energy range. The solar flares responsible for these flux increases are listed in Table 5. We are not certain of the origin of the flux increases (d) and (g); however, both are associated with the passage of shock fronts as identified by Forbush decreases and geomagnetic storm sudden commencements (see Figure 4).

Table 5 includes the transient characteristics of these solar proton events. These events display (1) short transit times and rise times in the 13 - 70 MeV energy range and (2) a time-dispersion effect between the first arriving fluxes at 13 - 70 MeV and 0.6 - 13 MeV. For example, we consider in detail the solar proton event (b) in Figure 4 and Table 5 which was produced by a solar flare in the eastern hemisphere of the Sun. We have measured the following characteristics:

1) The differential energy spectrum (Figure 12) was derived from energy-loss vs. range measurements. The particles are protons--not electrons--with a typical flare spectrum, $\frac{dJ}{dE} = 1.8 \times 10^{7} E^{-5}$ protons/m^2 sec ster MeV.

2) Figure 13(a) displays the directional distribution of the flux for 13-70 MeV protons. Averaged over four hours, the direction of maximum intensity is $\sim 20^{\circ}$ West of the Sun-spacecraft line with an anisotropy of $\sim 2.5:1$ with respect to the antisolar direction (after quiet-time background has been subtracted).

3) The time-dispersion effect for first-arriving particles within the energy range 0.6-70 MeV shows that this is a flare-produced event and not the entry of the spacecraft into a co-rotating region containing an enhanced proton flux which had been present for an extended time.

4) The maximum transit times (Table 5) from the flare region to the spacecraft are 120 minutes and 215 minutes for the 13-70 MeV and the 0.6-13 MeV energy protons, respectively. The time to propagate along the spiral magnetic field line from the point Y in the corona (see Figure 11) to the spacecraft at (b) is at least 25 minutes for $\leq$ 70 MeV protons and at least 60 minutes for $\leq$ 13 MeV protons. This means that the protons must have propagated in the corona from the flare site to the vicinity of Y in less than $\sim$ 90 and $\sim$150 minutes, respectively.

The characteristics of event (b) also prevail for events (a), (e) and (f), especially the existence of a large unidirectional anisotropy from a direction west of the Sun-spacecraft line. As an example, in Figure 13(b) we show the directional distribution

of 13-70 MeV protons for event (e) when the active center is $\sim 40^{\circ}$ West. This anisotropy of 14:1 illustrates the extreme collimation and smooth interplanetary magnetic field conditions at this time (Simpson, 1966).

It is difficult after 24 March to measure the characteristics of the additional small proton events from flares in region 8207 because a high ambient proton flux from event (f) persists for several days. For example, proton intensity increases similar in magnitude to events (a) or (b) (< 0.07 counts/second) barely would be discernible above the ambient flux in Figure 4 for 24-27 March. However, on 28 March an importance 2 flare was associated tentatively with proton event (h) (Table 4) when the active center was passing over the west limb of the Sun. This event has a transit time of $\sim$ 70 minutes and a directional anisotropy of 1.5:1 with maximum flux from $\sim 40^{\circ}$ West of the Sun-spacecraft line. Thus, the experimental evidence suggests that discrete proton events with short transit times in the energy range 13-70 MeV are observable from flares in region 8207 at least as far west as 90° under conditions similar to the proton events (a) . . . (f).

As we pointed out earlier this was a particularly simple period to analyze. There are other periods when the physical conditions are apparently much more complicated. For example, in some periods during December 1965 and January 1966, 13-70 MeV protons from flares display long transit times and very slow rise times. On the other hand, late in April and early in May we have evidence that discrete flare-produced proton events behave in a manner similar to that which we observe for the period of March 1966. However, because the data in May suffer from incomplete telemetry coverage, they do not provide as continuous and clear-cut a case for analysis as the March events.

E. Interplanetary propagation of 13-70 MeV protons from the flare of 24 March 1966.

In order to examine the propagation of solar protons from their emergence at the upper corona to their escape from the inner solar system, we have analyzed the proton event of 24 March 1966: event (f) in Figure 4 and Table 5. The optical flare began at 0225 U.T. at 42° West, and thus was almost directly beneath the position at which the interplanetary magnetic field extends from the corona to the vicinity of the spacecraft. Due to the large flux produced by this flare we have used quadrant counting rates (Section II and Appendix II) to analyze the directional distribution of protons arriving at the spacecraft. In Figure 14 we note that the counting rates of both the total intensity and Quadrant 2 (solar direction) begin to increase immediately after the optical flare begins. The energy-loss vs. range measurements indicate that the particles arriving at this time were electrons. Lin and Anderson (1967) have also observed a very large flux of solar electrons at this time. The data first indicate the arrival of protons at ~ 0250 U.T.; these first arriving protons are observed only in Quadrant 2. By 0300 U.T. the electron contribution to the total intensity is negligible in comparison with protons. We have indicated the period in which the electron contribution is significant by the dashed portion of the Quadrant 2 counting-rate curve in Figure 14. It is important to note that, at least in the initial phase of propagation, these electrons display a strong anisotropy similar to that observed for flare protons.

After the first indications of proton arrival, the Quadrant 2 counting rate increases rapidly and by 0310 U.T. it is too high to measure with the quadrant counter. Note that a significantly lower counting rate is observed in Quadrants 1 and 3 (East and West directions respectively) and that the counting rate in Quadrant 4 (antisolar direction)

is still lower. We interpret these facts to indicate that protons are propagating from the solar direction at low pitch angles and with very little scattering in the region between the Sun and the spacecraft. The comparatively low flux from the antisolar direction indicates that little scattering occurs for a significant distance beyond the orbit of the spacecraft. However, a measurable flux is observed from the antisolar direction within a few minutes of the arrival of protons from the solar direction.

At later times (> 0930 U.T.) the counting rates have decayed to a level at which we can again analyze the directional distribution. We find that the proton flux gradually approaches a persistent anisotropy after ~ 1300 U.T. with maximum flux arrival from a direction $0-20^{\circ}$ west of the Sun-spacecraft line. The decay phase of the event (see Figure 4) is better represented by an exponential decay law rather than a power law. We interpret these results as evidence that (a) equilibrium has been reached, with the steady-state anisotropy of < 10% which is probably due to co-rotation effects, and (b) that the characteristic time constant, τ , for the observed exponential decrease of observed flux is determined mainly by the interplanetary magnetic field irregularities beyond the orbit of the spacecraft. Since the decrease of intensity is exponential, the depth of the diffusion region must be finite (Meyer, Parker and Simpson, 1956) for protons in the 0.6-70 MeV energy range, i.e. the number of protons escaping is proportional to the number present in the region of space accessible to observation.

VI. MODELS FOR PROTON PROPAGATION WITHIN THE SOLAR CORONA

We have shown that 13-70 MeV protons from discrete solar-flare events have access to the interplanetary magnetic field high in the corona over a solar longitude range of ~ 100 degrees, and that the 0.6 to 13 MeV protons associated with solar active

centers have access to fields over a longitude range of ~ 180 degrees, more or less centered on the ~ 100 degrees range for the discrete flares. Since our measurements do not reveal directly how these protons reach the upper corona, it is our purpose in this section to discuss possible models to account for our observations.

Observations of discrete solar flare proton events place severe constraints on possible modes of propagation from the flare site to the upper corona. We begin with a discussion of the initial phases of the March 1966 flare events (a) . . . (h). To obtain the observed transit and rise times for the flare events in Table 5 we have assumed that protons are accelerated at the onset time of the associated 10-centimeter radio burst. We assume that for a given energy interval, e.g. 13 to 70 MeV, the first-arriving protons are at the high end of the energy range, i.e. 70 MeV, and that velocity dispersion between the high and low ends of the energy interval determines the rise time to maximum intensity. We note in Table 5 that the transit times for events (a) . . . (f) tend to decrease less than a factor of 2 as the relative longitude decreases from ~ 70° to ~ 0° between the flare site and the position in the upper corona from which the protons travel in space to the observer. The corresponding rise times of 13-70 MeV protons also vary by less than a factor of 2 but with no systematic dependence on the relative longitude of the flare site. Hence, for the following discussion we shall adopt the average values of these characteristic times.

The observed transit time is composed of two parts: the time in the corona and the time to propagate from the Sun to the spacecraft. The latter time is reasonably well-established since we know the energy of the protons and, from the strong anisotropy, their path in space. The time for transit along the archimedes spiral line is $\geq$ 25 minutes for 70 MeV and $\geq$ 60 minutes for 13 MeV protons (these times are lower limits since we are

assuming propagation with zero pitch-angle). The observed total transit times for these energies are ~ 110 and ~ 200 minutes and therefore, protons in the energy range 13 - 70 MeV spend at most 85 to 140 minutes in the corona.

However, isotropic diffusion in the solar corona does not appear to account for these data. For example, Reid (1964) has carried out detailed calculations on the diffusion of 130 - 600 MeV protons in the solar corona. For diffusion path-lengths of ~ 2 solar radii he arrives at rise times of at least 60 minutes. Our observations at lower energies (13 - 70 MeV) produce rise times of ~ 40 minutes of which at least 25 minutes can be attributed to a velocity dispersion effect in interplanetary space. It is also interesting to note that the rise time is essentially independent of the flare longitude for events (a), (b), (e), and (f) in Table 5.

There are indications, however, that isotropic diffusion may play an important role at later times. For example, in event (f) the main flux is directed from the Sun along the spiral magnetic field for several hours, namely ~ 0400-1100 U.T. in Figure 14. Assuming that high-energy proton acceleration at the flare site has stopped, some of these protons must be held up in the corona for many hours to account for this anisotropy. Similarly, diffusion may be an important factor at all times for some events such as (h), which displays long rise times in comparison with the other solar events in Figure 4.

In view of these factors we are convinced that, although isotropic diffusion would play an important and possibly dominant role in the late phases of these events, there must be a relatively fast propagation mode which guides the protons to the upper corona through a large longitudinal range. Anisotropic diffusion appears to be the most likely candidate. Hence, in our sketch in Figure 11 we have drawn magnetic lines of force connecting the solar active center and the flare sites to the magnetic field in the

upper corona which extends into space (at the dashed line) over the solar longitude range of ~ 100 degrees. It should be understood that these lines within the corona represent the general direction of the field, but that, in fact, the detailed magnetic field must be irregular.

We have pointed out that the transit and rise times are not strongly dependent upon the longitude of the flare site. This fact is in disagreement with isotropic diffusion models (Reid, 1964). Furthermore, the amplitude of the observed proton flux varies by orders of magnitude for solar flares with comparable radio and optical emission. This effect may be interpreted qualitatively as an "efficiency" for solar protons to reach the upper corona ~ 50° West. This efficiency rises from below threshold on 19 March to a maximum on 24 March as the flaring region moved from 30° East to 42° West. A similar effect has been observed by O'Gallagher and Simpson (1966) from simultaneous measurements on the Mariner-4 and IMP-3 spacecraft for proton flare events in 1965.

We now turn to the propagation in the solar corona of 0.6 to 13 MeV protons associated with a major solar active center. The magnetic field configurations required to explain proton propagation through the corona depend upon the assumptions we make regarding location of proton acceleration at the Sun. For example, if the protons were accelerated over a large fraction of the visible solar disk, they would propagate by diffusion to the upper corona without requiring special magnetic field configurations and would produce the observed distribution of enhanced flux in space over a large longitudinal range. However, there is no evidence to support acceleration over such an extended area. Indeed, our results point convincingly to solar active centers as the source of these protons; it appears that the observed enhanced flux of 0.6 - 13 MeV protons which has its onset on 15 March (Figure 6) originates in the frequent subflares

and discrete large flares from this center. The "integrating" effect of the frequent, small solar events would account for the more or less continuous flux of low-energy protons which increases as the active center moves towards the western hemisphere. Superposed on this enhanced flux would be the 0.6 - 13 MeV flux from the larger solar events such as (a) . . . (f).

We already have invoked magnetic fields extending from the active centers to the upper corona over a 100 degree longitude range to account for the discrete solar flare events. Therefore, we may either (a) extend this model to spread out further the connecting fields to 180 degrees for the 0.6 - 13 MeV protons, as illustrated in Figure 11, or (b) we may assume that these low-energy protons diffuse laterally in the corona beyond the propagation region for protons from discrete flares. Alternative (b) is merely an extension of the diffusion processes which go on at late times in the propagation of solar flare protons. Impulsive inputs of proton fluxes would be smoothed out by diffusion so that we would observe only gradual proton flux onsets as a result of a quasi-stationary flux distribution in space co-rotating with the Sun.

Alternative (a) on the other hand would make it possible to account for the apparent "horizon effect." That is, to account for proton flux onset and cut-off the magnetic field lines would extend approximately 90° in longitude eastward and westward from the solar active center. The archimedes spiral of the magnetic field in space would produce $\sim$ 45 degrees of rotation eastward so that the onset and cut-off appear when the center is $\sim 45^{\circ}$ and $\sim 135^{\circ}$ West of the observer as indicated in Figure 11.

An extended distribution in the corona of magnetic field from an active center might result from superheated plasma over the center spreading laterally in all directions and transporting the magnetic field over a wide range of longitudes. This

field begins to undergo co-rotation within a few solar radii above the photosphere, and within several solar radii takes the form of an archimedes spiral. This picture is not inconsistent with coronal optical observations. Isophotes of coronal streamers extending far above active centers have been described in detail by Newkirk (1966). Parker (1963; 1964) has pointed out on the basis of optical emission from the coronal gas that the magnetic lines of force in the region of coronal streamers may be nearly orthogonal to these isophote lines. The resultant field configuration is somewhat similar to the one we suggest. Based on the preliminary solar-wind velocities measured by J. Wolfe (private communication) on the Pioneer-6 spacecraft, we find that the peak in the velocity distribution is sufficiently sharp to resolve the appearance of region 8207 as it passes across the solar disk, that is, the highest-velocity solar wind is measured at the spacecraft when the active center is 3 to 4 days beyond central meridian. The period of enhanced solar wind velocity is comparable to the period of enhanced low-energy proton flux.

The total magnetic flux distributed in interplanetary space for this model is readily supplied by typical solar active regions. For example, the integral flux over a heliocentric longitude range of $\sim 180^{\circ}$ (assuming $\pm 90^{\circ}$ latitude spread as an upper limit) with an average interplanetary field intensity of 2×10^{-5} gauss at the spacecraft leads to a field intensity of 100 gauss distributed over an active center of diameter $\sim 10^{5}$ km on the photosphere. This value of magnetic field intensity appears to be compatible with observations.

Although the model we have discussed above satisfies many of the observations there exists at least one possibility for explaining the presence of the 0.6 to 13 MeV proton flux beyond the region in the corona which is directly accessible to solar flare protons of higher energies. It has been pointed out (Simpson, 1963) that a compo-

nent of the low-energy protons observed in interplanetary space may originate in the decay of solar neutrons near the Sun. If neutron production occurred near the photosphere in a solar active center (e.g. from subflares) the neutron trajectories would display a "horizon effect." However, there is evidence (Section VII) that features of the low-energy proton flux profile are associated with interplanetary magnetic field features (e.g. sector boundaries, or terminations of the Forbush decrease effect). Thus these features are not consistent with uniform decay of neutrons over the whole solar hemisphere. Further work will be required to decide whether or not there is an alpha-particle component associated with these low-energy protons, and whether the horizon effect is independent of energy and intensity, before positive evidence for a significant contribution of protons from neutron decay can be obtained.

VII. EVIDENCE FOR LARGE-SCALE STRUCTURE OF INTERPLANETARY MAGNETIC REGIONS

Our description of a large-scale magnetic region in interplanetary space associated with a solar active center has been based upon our study of solar proton propagation. We now examine the independent evidence available to us for the existence of these large-scale magnetic regions.

A. Pioneer-6 Sector Boundaries

Recently Ness (1967) has made available the approximate times for crossing magnetic sector boundaries--a boundary is defined as the transition from a magnetic region of one polarity to an adjoining region with the opposite polarity (Ness and Wilcox, 1965). The boundaries derived from his magnetometer observations on Pioneer-6 from December 1965 through April 1966 reveal the following general characteristics:

a) A sector boundary passed the spacecraft within 24 hours of the proton flux onsets on 25 December 1965, 13 January 1966, 15 March 1966 and 31 March 1966 (Table 4).

b) A sector boundary passed within 3 days of the proton flux cut-offs on 4 January 1966, 28 January 1966, 31 March 1966, and 10 April 1966.

c) If we set aside the boundary identifications which occur during the shock waves from solar flares in the intervals 20 - 22 January and 23 - 25 March 1966, we conclude that single sectors occupied most, but not necessarily all, of the magnetic regions derived from the proton flux measurements. Three sectors were (+) polarity and the fourth sector was (-) polarity (31 March - 9 April).

A similar correlation was obtained in 1963 - 1964 with the IMP-I satellite between 27-day recurring fluxes of 1 MeV protons (Fan, Gloeckler, and Simpson, 1965), and co-rotating magnetic sectors (Ness and Wilcox, 1965). It is important to note that the IMP-I results also showed that these flux increases often exceeded the sector-boundary limits by a few days.

The relation of IMP-I interplanetary magnetic sectors to the calcium plage structures found by Wilcox and Ness (1967) suggests that the phenomena observed in 1963 - 1964 are qualitatively the same as we now find from the Pioneer-6 and Pioneer-7 analysis under the assumption that the magnetic regions have greatly expanded during the increasing phase of the solar activity cycle.

B. Modulation of Galactic Cosmic Rays

We may deduce some of the large-scale properties of the magnetic region

shown in Figure 11 from the fact that both quasi-stationary magnetic field structures and shock waves from solar flares produce the well-known modulation of cosmic rays as measured by neutron intensity monitors (Fan, Gloeckler, and Simpson, 1965, and references therein). Our examples are taken from Figures 4 and 5 where we show cosmic-ray intensity changes measured by the Climax neutron monitor, for protons $> \sim 3$ GV magnetic rigidity.

There are two outstanding effects which we note here:

1) Upon entering the magnetic region as defined by the appearance of the proton flux onsets (15 March and 22 August) we find that cosmic-ray modulation becomes observable within 50 hours. This modulation effect, which occurs before the large-scale Forbush decrease we report below, is similar to that studied by Legrand (1960).

2) Within an interplanetary magnetic region containing solar protons a shock wave from a solar flare may pass the observer and produce a large Forbush decrease. Examples of this large-scale galactic modulation of cosmic rays are shown in Figures 4 and 5 on 23 March and 30 August. This modulation continues until 1 April and 8 September, respectively, at which time there is an abrupt decrease in the degree of modulation. Since the solar proton cut-offs occur at nearly the same times we believe that the large-scale features of the magnetic field which define the longitudinal limits of galactic cosmic-ray modulation are the same general features which influence the longitudinal spread of solar protons at the corona. At this time the shock wave is several A.U. beyond the spacecraft, so that these

regions must extend over comparable distances into the solar system. Indeed, from the simultaneous observations of Pioneer-7 and IMP-3 on 8 September we find that the observed proton intensity profile at the cut-off co-rotates with the Sun (note that the time at which co-rotation is observed is identified in Figure 5 by the symbol x). We call attention to the fact that the proton flux in the 0.6 - 13 MeV range dropped a factor of 5, indicating the isolation of adjacent regions.

From our observations we cannot decide whether or not shock waves are required for the formation of these regions. However, there is the possibility that a series of shock waves from major solar outbursts may play an important role in the formation of quasi-stationary magnetic regions spreading over 180 - 200 degrees of longitude. This might account for the nearly symmetrical character of the magnetic regions with respect to the location of the solar-active centers which we have studied in this paper. That is, the apparent longitudinal spread in the corona of the solar low-energy protons and the magnetic region to ~ 90 degrees to each side of the active center might follow naturally from the geometry of shock wave phenomena to produce an apparent "horizon effect" at the Sun.

C. Escape of Solar Protons from the Interplanetary Magnetic Field Regions.

By investigating the decay of solar proton fluxes from magnetic regions accessible to the spacecraft, some important conclusions may be drawn regarding the characteristics of the distant interplanetary magnetic field. For example, the instantaneous proton flux measured at the spacecraft after intensity maximum is determined both

a) by the rate at which protons are being released from the upper corona after the flare event, and b) by the rate at which the observed protons can escape by diffusion through magnetic irregularities in the interplanetary field beyond the orbit of the spacecraft.

During the initial phase of solar flare proton propagation the flux level in the region of space accessible to the observer is dominated by the anisotropic propagation from the solar corona. However, at late times we have shown in Sec. V that the anisotropy decreases to less than 10% and the characteristics of the interplanetary field determine the rate of proton-flux decay. At late times an outstanding feature of the proton flux time-dependence is the exponential form of the decay. Typical examples are found in the semilogarithmic plots of Figures 2, 3, 4 and 5. We have found eight intervals over an eight-month period where exponential decreases were measured simultaneously in the two energy intervals 0.6 - 13 MeV and 13 - 70 MeV under the constraint that the observations extended over a time interval $> 1.5\ \tau_o\ (0.6 - 13)$ where $\tau_o\ (E_1 - E_2)$ is the exponential decay constant for protons in the energy interval $E_1 - E_2$. As shown in Table 6 the range of values for τ_o and the range of the ratio $\tau_o\ (0.6 - 13) / \tau_o\ (13 - 70)$ is less than a factor of 3.5 for all of the events. Hence the characteristics for solar proton escape from the inner solar system do not change drastically during the eight-month period.

VIII. SUMMARY AND REMARKS

A. Association of solar protons with active centers.

1) We have found enhanced fluxes of protons with energies 0.6 - 13 MeV continuously present in the interplanetary magnetic field over a solar longitude range of ~ 180 degrees and have shown that these protons have their source at the Sun. These fluxes occur in association with solar active centers which continually produce

subflares in addition to frequently occurring larger flares, which are identified by optical and radio emission. Figure 7 summarizes these intervals of enhanced flux and the positions of the associated solar active centers. We find no arguments requiring interplanetary acceleration to account for these particles. There is the possibility that the > 1 MeV protons observed in 1963 - 1965 by Bryant et al. (1965) and Fan et al. (1965) may be of subflare origin in weak active centers not so far identified.

2) We use this proton flux to trace the portion of the interplanetary magnetic field which is connected with the solar source, thereby identifying the longitudinal extent of the magnetic field regions in the vicinity of the ecliptic plane. We find from the sector boundaries detected by the magnetometer on Pioneer-6 (Ness, 1967) that single sectors occupy most, but not necessarily all, of the magnetic region associated with the proton fluxes.

3) The regions of interplanetary magnetic field within which these protons propagate are isolated from adjacent regions in which the enhanced solar proton flux is often absent for several days, or where the flux from a different active center is present.

4) Superposed on the enhanced flux of 0.6 - 13 MeV protons are discrete flare events which are also observable in the energy range 13 - 70 MeV. However, these discrete events are detected over a solar longitude range of ~ 100 degrees, which is substantially less than the ~ 180° range observed for the enhanced flux. Consequently we find that this enhanced flux of ~ 1 MeV protons will appear a few days before the first observable event at higher energies.

5) We have proven that the particle phenomena we are investigating are due to protons--not solar electrons--by detailed measurements of the differential

energy spectra using particle energy-loss and range. Furthermore, by analyzing the arrival directions of protons from discrete solar flares we have shown that, soon after the flare, the protons propagate from the Sun along the average interplanetary magnetic field direction. This field leaves the solar corona at ~ 50° West longitude.

6) Discrete proton flux increases in the energy range 13-70 MeV from solar flares as far East as 30° longitude are observed to arrive from a direction ~ 20° to 45° West of the Sun-spacecraft line ~ 100 minutes from the start of the parent flare. The flux then rises to its maximum level in ~ 40 minutes. These short times lead us to conclude that, although some diffusion of 13-70 MeV protons in the corona is likely to occur, isotropic diffusion does not play the major role in the initial stage of propagation within the corona.

7) We can fulfill the conditions required by both (a) the continually present 0.6-13 MeV flux over ~ 180° longitude, and (b) the discrete solar proton observations by assuming that the magnetic field lines from a solar active center are spread out over 180 degrees of solar longitude in the corona by the superheated coronal gases from over the solar center, as shown in Figure 11. This quasi-stationary model results in a longitudinal distribution of magnetic field which is then carried into interplanetary space by the solar wind. We note that this model appears to be consistent with observations of coronal streamers extending several solar radii above an active center.

B. Proton propagation in the interplanetary medium.

Although the study reported in this paper was directed to the large-scale properties of proton propagation in space and in the corona, we have observed several important effects which describe, in detail, proton propagation in interplanetary space.

These effects are:

1) The first-arriving protons from a solar flare display strong unidirectional anisotropies with maximum flux from the average interplanetary magnetic field direction, approximately 45° west of the Sun-spacecraft line. We conclude that there is negligible scattering of 13-70 MeV protons between ~ 0.3 A.U. (for a typically observed pitch-angle distribution) and the spacecraft located at ~ 1 A.U.

2) Significant scattering in magnetic fields occurs beyond the location of the spacecraft. We have observed the gradual return of solar proton flux from the antisolar direction. This return is detectable within a few minutes of the detection of flux from the solar direction, but at a much reduced amplitude.

3) After a major solar proton event has attained maximum intensity we find that the directional anisotropy asymptotically approaches a value of $\leq$ 10 percent from a direction slightly west of the Sun-spacecraft line. This anisotropy is likely to find its explanation in the combined effect of the co-rotating magnetic fields and the persistent gradient of flare proton flux in the inner solar system. We also note that at late times the proton flux observed at the spacecraft decreases exponentially with an energy-dependent time constant which varies less than a factor of 3.5 for discrete events over an 8-month period. We conclude that this observed exponential decay is determined by interplanetary magnetic field conditions beyond the orbit of Earth and within the longitudinal range of the magnetic region connected with the active

center. Storage of particles in magnetic fields at the Sun does not play a major role in the decay phase except for the first few hours after the flare.

4) For the first time we have obtained the directional distribution for protons down to 0.8 MeV. The quiet-time flux at this energy is isotropic to within $\sim$ 5%.

5) The gradual onsets of enhanced low-energy flux are strongly anisotropic in the energy range 0.8 - 2 MeV with the maximum flux arriving from a direction $\sim 30 - 40^{\circ}$ west of the Sun-spacecraft line.

6) We find evidence for interplanetary shock waves producing proton intensity increases. We shall defer reporting on the detailed analysis of these events to a later publication. However, since we observe that low-energy protons $\gtrsim$ 1 MeV present in the interplanetary medium before the shock are still present at the same flux levels after passage of the shock, we believe the acceleration is either adiabatic or, in any case, not important for the principal phenomena discussed in this paper.

Although the above interplanetary phenomena are taken from only a few examples we believe these properties of solar proton propagation to be quite general in the period of nine months following the appearance of major active regions in the new solar cycle.

C. Concluding remarks.

The question naturally arises as to what effect the energy threshold (0.6 MeV) and the threshold for flux increases ($\sim 10^{-3}$ particles/cm^2 ster sec) have for defining the

longitudinal extent of these magnetic regions associated with active centers. A further reduction of energy threshold would reveal more details regarding the cut-off observed in the 0.6 - 13 MeV enhanced proton fluxes. Some periods of enhanced flux do not exhibit sharp cut-offs (e.g. 1 - 10 April 1966) but show slow declines to background. Since at low flux levels the differential energy spectrum is $\sim E^{-3}$, a further reduction of energy threshold would reveal whether all major solar active centers have a characteristic flux cut-off of $\sim 130^{\circ}$ West. If so, this would strengthen the point of view that this limit is a solar "horizon" effect.

We wish to re-emphasize that the period of observations for the Pioneer-6 and Pioneer-7 space probes was coincident with the appearance of the first major active centers of the solar cycle. The observations began at the time (December 1965) solar modulation of the galactic cosmic rays was within 1 - 2 percent of the minimum of May 1965 (Wang and Simpson, 1967) so that the shock waves from solar flares within the period of Pioneer observations are the first major contributors to large-scale modulation in the solar cycle. The relatively simple solar conditions and modest proton flux levels which existed for most of our observations cannot be expected to continue into 1967. Indeed, during September 1966 there were already some difficulties developing in interpretation due to the complexity of solar activity.

The solar active centers responsible for the principal flare activity from December 1965 through mid-1966 were located in two principal longitude regions on the Sun approximately 180 degrees apart. Apparently the same solar longitude regions were observed for the two principal flaring regions in the last solar cycle (No. 19) from 1960-1963 (Guss, 1964; Sakurai, 1966). If this correlation is maintained in the future it is likely that major active regions have their origin in semi-permanent magnetic structures

in the photosphere.

Finally, we point out that the role of a super-heated coronal plasma in spreading the magnetic fields from the active center, as suggested by our model, is not understood. The proton data, however, provide the first evidence for the connection of these magnetic fields with the interplanetary medium.

In the final stage of drafting this paper we have received a preprint by McCracken, Rao and Bukata (July 1967) on their analysis of solar flare events, also using particle detectors on Pioneer-6 and Pioneer-7 which have a low-energy threshold for protons of 7.5 MeV. Although they do not measure directly differential energy spectra and thereby do not separate electrons and protons, there appears to be essential agreement on the propagation behavior for protons. However, due to their high energy threshold they observe only the discrete events which we find in our high-energy channels, shown in Figure 2.

ACKNOWLEDGMENTS

We are grateful to the staff of the Laboratory for Astrophysics and Space Research of the Enrico Fermi Institute for Nuclear Studies (especially to J. Lamport, R. Weissman, R. Jacquet and E. Grokulsky) for their contributions to the management, design, construction and testing of the Pioneer-6 and Pioneer-7 instruments. We thank G. Lentz and R. Hermon for the development of computer programs for the preparation of data, and D. Gerhart and D. Morrison for assistance in data analysis. A. Tuzzolino, J. Kristoff and M. Perkins were responsible for the excellent, large-area solid-state detectors. We gratefully acknowledge the efforts of the Pioneer Project staff at Ames Research Center (especially C. F. Hall, J. E. Lepetich, H. Cross, R. Nunamaker, A. Natwick, and C. Frosolone) in the pre-launch testing, flight operations, and preliminary data preparation. We

appreciated the contribution of R. Tjonaman in supervising the Climax neutron monitor operations. It is a pleasure to thank N. Ness for a preliminary survey of his magnetometer data on Pioneer-6, J. Wolfe of Ames Research Center for supplying preliminary solar-wind velocities from the Pioneer-6 spacecraft, and the Meudon Observatory for permission to use their solar charts in advance of publication. Finally, we appreciated receiving helpful comments on this manuscript from E. N. Parker, K. B. Fenton and J. J. O'Gallagher.

This research was supported in part by the National Aeronautics and Space Administration under contract NAS 2-1758 and grant NsG 179-61, and by the Air Force Office of Scientific Research under contract No. AF 19 (638) 1642.

APPENDIX I

List of References for Solar Activity

Optical Flares:

1. Quarterly Bulletin on Solar Activity, Meudon Observatory, France.
2. CRPL (Part B), Space Disturbances Laboratory, Solar-Geophysical Data, U.S. Department of Commerce, Boulder, Colorado, U. S. A.

Radio Bursts:

1. Quarterly Bulletin on Solar Activity, Meudon Observatory, France.
2. CRPL (Part B), Space Disturbances Laboratory, Solar-Geophysical Data, U. S. Department of Commerce, Boulder, Colorado, U. S. A.
3. Solar Radio Noise Measurements, NERA, Netherlands.
4. Solar Radio Emission, Toyokawa, Japan.

Centers of Activity:

1. Charts with isophotes of the 5303 Å coronal emission line, Quarterly Bulletin on Solar Activity, Meudon Observatory, France.
2. Synoptic charts of the solar chromosphere, Meudon Observatory, France.
3. Solar radio emission spectroheliograms at 10 cm, Stanford University, California, U. S. A.

APPENDIX II

Measurement of Proton Anisotropy

The directional information consists of the sector identification of each particle which is pulse-height analyzed. By means of the pulse-height information particles may be selected for directional analysis according to energy and species. The sector-distribution of particles detected during a specified time interval is fitted by a least-squares technique to an expression of the form

$$F(\theta) = A + B\sin(\theta + \varphi_1) + C\sin 2\cdot(\theta + \varphi_2) \qquad (1)$$

where F is particle flux (particles per cm^2 ster sec) and θ is the angle in the ecliptic plane measured westward from the Sun-spacecraft line. A, B, C, φ_1, and φ_2 are constants determined by the fitting technique, which includes the effect of the telescope geometry. In those cases where the first two terms of (1) provide a good fit to the observed sector distribution the degree of anisotropy may be characterized by the ratio B/A (expressed as a percentage) and the direction of maximum flux may be determined from φ_1.

However, in those cases in which the distribution of events in the eight sectors is highly peaked, then (1) may not give an adequate representation of the distribution of particle flux. In these cases (e.g. Table 5) a better approximation is obtained by using the ratio of the number of events in the four sectors containing the peak to the number of events in the four sectors in the direction of minimum flux. This procedure for indicating the degree of anisotropy is also used when the number of particles detected is insufficient to ensure a statistically good fit to expression (1).

The maximum event rate for which our instrument can analyze the directional distribution and species of a particle flux by sectors is determined by the telemetry transmission rate from the spacecraft. That is, the sector indication and energy-loss of at most one particle event may be transmitted per telemetry interval (0.4375 - 28.0 seconds, depending upon transmission rate).

An increase in the maximum event rate usable for directional analysis is obtained by counting the number of $D_1 D_2 \bar{D}_3 \bar{D}_4$ coincidence events (see Table 1) occurring in each of four quadrants, with each quadrant consisting of two sectors (see inset in Figure 14). The number of events is accumulated and transmitted for each quadrant sequentially. It should be emphasized that a unique identification of particle species is not possible from the quadrant counts alone since only a particle range measurement is performed (i.e. only $D_1 D_2 \bar{D}_3 \bar{D}_4$ coincidence events are accepted). However, the pulse-height information may be used to determine the average composition and energy spectrum of the flux. Quadrant analysis of the directional distribution can be done for event rates at least a factor of 16 greater than the maximum event rate usable for sector analysis. The quadrant counting rates are especially useful during solar flares, as shown in Figure 14.

REFERENCES

Avignon, Y. and M. Pick, Relation entre les émissions solaires de rayons cosmiques et les surtauts de type IV, Comp. Rend. Ac. Sc., 249, 2276-2278, 1959.

Bryant, D. A., T. L. Cline, U. D. Desai and F. B. McDonald, Continual acceleration of solar protons in the MeV range, Phys. Rev. Letters, 14, 481-484, 1965.

Caroubalos, C. A., Study of the slowly varying component at three centimeters as a function of solar activity, Solar System Radio Astronomy; National Observatory of Athens, Greece, 109-116, 1964.

Fan, C. Y., G. Gloeckler, K. C. Hsieh, and J. A. Simpson, The isotopic abundances and energy spectra of He^3 and He^4 above 40 MeV per nucleon from the galaxy, Phys. Rev. Letters, 16, 813-817, 1966.

Fan, C. Y., G. Gloeckler, B. McKibben, K. R. Pyle, and J. A. Simpson, Differential energy spectrum and intensity variations of 1 - 20 MeV/nucleon protons and helium nuclei in interplanetary space (1964-1966), Proc. Tenth Int. Conf. on Cosmic Rays, Can. J. Phys., 1968 (in press).

Fan, C. Y., G. Gloeckler, and J. A. Simpson, Conference on initial results of IMP-I satellite, Goddard Space Flight Center, March, 1964.

Fan, C. Y., G. Gloeckler, and J. A. Simpson, Proc. Ninth Int. Conf. on Cosmic Rays, Accel. 3, Vol. 1, 2, 109-111, The Physical Society, London, 1966.

Fan, C. Y., J. E. Lamport, J. A. Simpson, and D. R. Smith, Anisotropy and fluctuations of solar proton fluxes of energies 0.6 - 100 MeV measured on the Pioneer-6 space probe, J. Geophys. Res., 71, 3289-3296, 1966.

Guss, D. E., Distribution in heliographic longitude of flares which produce energetic solar particles, Phys. Rev. Letters, 13, 363-364, 1964.

Hakura, Y. and T. Goh, Unusual solar-terrestrial events in July 1959, Space Research II, 803-812, 1961.

Krimigis, S. A. and J. A. Van Allen, Observation of ~ 500 kev protons in interplanetary space with Mariner IV, Phys. Rev. Letters, 16, 419-423, 1966.

Kundu, M. R., Structures et propriétés des sources d'activité solaire sur ondes centimétriques, Ann. d'Astrophys., 22, 1 - 100, 1959.

Kundu, M. R., and F. T. Haddock, A relation between solar radio emission and polar cap absorption of cosmic noise, Nature, 186, 610-613, 1960.

Legrand, J. P., Les prébaisses de rayons cosmique en période de maximum de l'activité solaire, Ann. d'Geophys., 16, 140-142, 1960.

Lin, R. P. and K. A. Anderson, Electrons > 40 kev and protons > 500 kev of solar origin, Solar Physics, 1, 446-464, 1967.

McCracken, K. G., and N. S. Ness, The collimation of cosmic rays by the interplanetary magnetic field, J. Geophys. Res., 71, 3315-3318, 1966.

McCracken, K. G., U. R. Rao, and R. P. Bukata, Recurrent Forbush decreases associated with M-region magnetic storms, Phys. Rev. Letters, 17, 928-932, 1966.

McCracken, K. G., U. R. Rao and R. P. Bukata, Cosmic ray propagation processes I: A study of the cosmic ray flare effect, preprint, July 1967.

Meyer, P., E. N. Parker, and J. A. Simpson, Solar cosmic rays of February 1965 and their propagation through interplanetary space, Phys. Rev., 104, 768-783, 1956.

Meyer, P., and J. A. Simpson, Changes in amplitude of the cosmic-ray 27-day intensity variation with solar activity, Phys. Rev., 96, 1085-1088, 1954.

Ness, N. F., Direct measurements of interplanetary magnetic field and plasma, IQSY/ COSPAR Symposium July 18, 1967, London, Preprint X-612-67-293.

Ness, N. F. and J. M. Wilcox, Quasi-stationary co-rotating structure in the interplanetary medium, J. Geophys. Res., 70, 5793-5805, 1965.

Newkirk, G., A. A. S. Symposium on Solar Physics, Boulder, Colorado, October 1966.

O'Gallagher, J. J. and J. A. Simpson, Anisotropic propagation of solar protons deduced from simultaneous observations by earth satellites and the Mariner-4 space probe, Phys. Rev. Letters, 16, 1212-1217, 1966.

Parker, E. N., Interplanetary Dynamical Processes, Interscience, New York, 1963.

Parker, E. N., Dynamical properties of stellar coronas and stellar winds III. The dynamics of coronal streamers, Astrophys. J., 139, 690-709, 1964.

Reid, George C., A diffusive model for the initial phase of a solar proton event, J. Geophys. Res., 69, 2659-2667, 1964.

Sakurai, K., The persistence of solar flare regions related to the production of energetic protons and interplanetary magnetic fields, Pub. Astron. Soc. Japan, 18, 350-356, 1966.

Simpson, J. A., Recent investigations of the low energy cosmic and solar particle radiations, Vatican Conference, Vatican City, 1963.

Simpson, J. A., A. A. S. Symposium on Solar Physics, Boulder, Colorado, October 1966.

Wang, J. and J. A. Simpson, Dimension of the cosmic ray modulation region, Astrophys. J. Letters, 149, L73-L78, 1967.

Wilcox, J. M. and N. F. Ness, Solar source of the interplanetary sector structure, Solar Phys., 1, 437-445, 1967.

Table 1

Charged-Particle Counting Rates and Analysis in the Pioneer-6 and Pioneer-7 Cosmic-Ray Telescopes

a	b		c	d	e	
Particle Range and Counting Rates	Kinetic Energy (MeV) Protons	Helium	Acceptance Cone Angle	Geometrical Factor (m^2 - sr)	Pulse-Height and Direction Analysis (8 Sectors) Pioneer-6	Pioneer-7
$D_1\bar{D}_2\bar{D}_4$	0.6-13	2.5-52	110°	5.8×10^{-4}	None	D_1 + only
$D_1D_2\bar{D}_3\bar{D}_4$ *	13-70	52-280	60°	1.15×10^{-4}	D_1 only	D_1 only
$D_1D_2D_3\bar{D}_4$	70-200	> 280	60°	1.15×10^{-4}	D_1 and D_3 ‡	D_1 and D_3 ‡
$\bar{D}_1D_2D_3\bar{D}_4$	> 200	None	60°	1.7×10^{-4}	None	None

* This counting rate also is divided into quadrants for anisotropy measurements.

+ Operates on command from Earth.

‡ Arrival direction determined below 120 MeV/nucleon only.

Table 2

Number of Days at Background for Solar Rotations 1812-1821[+]

Rotation No.	0.6 - 13 MeV[‡]	13 - 70 MeV
1812	5	20
1813	7	26
1814	16	27
1815	4	17
1816	2 - 6	18
1817	2	23
1818	*	*
1819	*	*
1820	>6	>6
1821	0	6

* Insufficient telemetry tracking coverage to determine level of activity.

[+] Solar rotations 1812-1817 are from Pioneer 6 data; 1820-1821 from Pioneer 7.

[‡] The entries correspond to the number of days on which the counting rate was below 0.2 counts per second.

Table 3

Significant Solar Active Centers

Identification Number	Carrington Coordinates		Date of Central Meridian Passage	Number of Optical Flares	Number of Radio Bursts at 10 cm	
	Lat.	Long.			Each center	Total for time on Disk
8105* (1502 07)+	10N	205	25 Dec. 1965	24	15	23
8110 (1502 11)	30S	118	31 Dec. 1965	6	1	
8131 (1503 09-10)	23N	228	19 Jan. 1966	24	11	~ 12
8133 (1503 14)	30N	200	21 Jan. 1966	3	1	
8207 (1505 05)	18N	146	21 Mar. 1966	143	125	155
8223 (1506 02)	28N	332	3 Apr. 1966	100	74	112
8240 (1506 06)	22N	288	7 Apr. 1966	20	9 (after 8 Apr.	
8240 (1506 06)	22N	288	7 Apr. 1966	33	14	17
8262 (1506 09	21N	135	18 Apr. 1966	31	26	37
8275 (1596 11)	29N	106	20 Apr. 1966	7	3 (after 24 Apr.)	
8272 (1506 14)	19N	62	23 Apr. 1966	11	4 (after 20 Apr.)	
8362 (1509 15)	35N	208	3 July 1966	57	21	30
8379 (1509 18)	22N	153	7 July 1966	14	4 (after 11 July)	
8413-8414 (1510 17-18-19-20)	27N	185	1 Aug. 1966	38	17	37
8408 (1510 11)	37N	270	26 July 1966	20	10 (before 26 July)	
9450-8461 (1511 17-18-19)	23N	190	28 Aug. 1966	43	59	96
8454 (1511 10)	07N	248	24 Aug. 1966	21	9 (before 28 Aug.)	
8496 (1512 04)	21N	348	12 Sept. 1966	12	7 (after 7 Sept.)	

* McMath plage number.

+ Identification number of Quarterly Bulletin on Solar Activity.

Table 4

Active Centers and Associated 0.6 - 13 MeV Proton Fluxes

Identification Number (McMath)	History of Plage Region	Spacecraft	Proton Flux Onset (day and heliographic longitude of solar center)	Proton Flux Cut-off (day and heliographic longitude of solar center
8105 (Figure 3)	Born on disk 24 December 1965	P-6	25 December 1965 0°	4 January 1966* 130° W
8131 (Figure 3)	Present at East Limb	P-6	13 January 1966 75° E	28 January 1966 130° W
8207 (Figure 4)	Present at East Limb (return of 8174)	P-6	15 March 1966 80° E	31 March 1966 130° W
8223 (Figure 4)	Present at East Limb (return of 8191)	P-6	31 March 1966 40° E	10 April 1966 90° W
8240	Present at East Limb (Increased flare activity after 7 April)	P-6	12 April 1966 60° W	15 April 1966+ 110° W
8262	Present at East Limb (return of 8207)	P-6	16 April 1966 45° E	22 April 1966+ 60° W
8362	Present at East Limb (develops rapidly after 30 June)	IMP-3	4 July 1966 5° W	> 14 July 1966+ $\geq$ 140° W
8413-8414	Present at East Limb (return of 8362 and 8373)	IMP-3	25 July+ 90° E	9 August 1966 110° W
8459-8461 (Figure 5)	Present at East Limb (return of 8327,8413,8414)	P-7	22 August+ 80° E	8 September 1966‡ 140° W

* A co-rotation effect was observed between IMP-3 and Pioneer-6 ~ 48 hours before proton cut-off.

+ Possible confusion with another center.

‡ Co-rotation of the proton cut-off was observed between IMP-3 and Pioneer-7.

Table 5

Discrete Proton Flare Events 15 - 30 March 1966

Event	Proton Intensity Increases in Figure 4						Associated Radio Bursts and Optical Flares					
	Transit Time from Sun to spacecraft (minutes)+		Rise time to maximum intensity (minutes)		Propagation Characteristics during onset (protons 13-70 MeV)		Date (1966)	Radio Onset (U.T.)	Duration (minutes)	Maximum Radio Flux*	Optical Flare Importance	Heliographic Longitude (degrees)
	13-70 MeV	0.6-13 MeV	13-70 MeV	0.6-13 MeV	direction	anisotropy‡						
(a)	106 + 5	143 + 5	47 + 10	305 + 65	30° W	1:8:1	19 Mar.	2140	50	5.6	1	E 15
(b)	119 + 10 102 + 10 80 + 10	214 + 20 197 + 20 175 + 20	35 ± 10 " "	~ 220 " "	20° W	2:1 see Fig. 13 (a)	20 Mar.	0954 1011 1038	17 22 23	1875 41 94	2 2	E 25 E 08
(c)	113 ± 15	-	~ 180	slow increase			21 Mar.	2230	4	33	2	W 10
(d)	-	-	-	-	20° W	bidirectional	Event (d) is associated with a shock front which gave rise to a Forbush decrease on 23 Mar.					
(e)	87 ± 5	Uncertain (152-236)	48 ± 10	Uncertain	10° W	12:1 see Fig. 13(b)	23 Mar.	2251	3	20	1	W 33
(f)	39 + 5 (> 300 MeV) (70 - 200 MeV) 35 + 5 (13-70 MeV)	152 ± 2	25 + 10 (> 200 MeV) (70 - 200 MeV) 43 + 5 (13-70 MeV)	70 estimated	10-20° W	unidirectional see Fig. 14	24 Mar.	0226	14	475	2	W 42
(g)	-	-	-	-	15°E	bidirectional	Event (g) is associated with a shock front which produced a sudden commencement on 27 Mar.					
(h)	70 ± 15	-	120 ± 30	-	40° W	1.5:1	28 Mar.	1415	105	8.8	2	W 90

* Maximum radio flux in units of 10^{-22} w/m^2 Hz at 10 cm.

+ Measured from onset of 10-cm radio burst (8 minutes have been added to correct for Sun-Earth transit time).

‡ Anisotropy defined as ratio of the number of protons in the four sectors centered on direction of maximum flux to the number of protons detected in the four sectors centered on direction of minimum flux.
Direction is measured with respect to Sun-spacecraft line.

Table 6

Characteristic Time Constants for Exponential Decreases of Proton Fluxes (January - September 1966)

Spacecraft	Time Interval (Mo/day/hour) Start	End	Energy Range (MeV)	τ_o (0.6-13) (days)	τ_o (13-70) (days)	$\frac{\tau_o(0.6\text{-}13)}{\tau_o(13\text{-}70)}$	Directional Anisotropy (%)	N *
P-6	1/2/16	1/4/12	0.6-13	0.47		0.8	$< 7^{\ddagger}$	3.9
	1/1/18	1/4/04	13-70		0.63^{+}			3.8
P-6	1/22/12	1/27/12	0.6-13	1.55		2.2	$< 5^{\ddagger}$	3.2
	1/19/12	1/21/06	13-70		0.70			2.5
P-6	3/25/12	3/31/12	0.6-13	1.1		1.7	8 ± 4	5.4
	3/26/00	3/28/00	13-70		0.87			2.3
P-6	5/9/00	5/11/12	0.6-13	1.2		1.7	22 ± 4	2.1
	5/6/18	5/8/00	13-70		0.70			2.1
P-6	6/25/18	6/27/18	0.6-13	1.26		1.8	16 ± 10	2.4
	6/26/00	6/27/00	13-70		0.7			1.4
P-7	8/31/00	9/02/00	0.6-13	1.3		0.9	9 ± 2	1.6
	9/01/00	9/02/00	13-70		1.5			0.7
P-7	9/5/14	9/10/12	0.6-13	1.4		1.4	2 ± 0.5	3.5
	9/5/12	9/11/00	13-70		0.91			4.6
P-7	9/15/00	9/19/06	0.6-13	1.65		1.2	4 ± 2	2.8
	9/15/12	9/19/06	13-70		1.33			1.5

* Number of factors of e over which the flux decreased exponentially.

$^{+}$ Possibly two components.

‡ Upper limit, determined by statistical considerations.

FIGURE CAPTIONS

Fig. 1 Cross-section view of the charged-particle telescope. The main axis of the telescope is perpendicular to the spacecraft spin axis and scans the ecliptic plane. Charged-particle energies and ranges measured with this telescope are given in Table 1.

Fig. 2 One-hour averages of the $D_1 D_2 \bar{D}_3 \bar{D}_4$ coincidence counting rate corresponding to the proton flux in the energy range 13 to 70 MeV. The data for solar rotation numbers 1812-1816 are from Pioneer-6. Pioneer-7 data are shown for solar rotation No. 1821. There are 19 solar proton events in this figure, identified by vertical arrows. The brackets ⌜——⌝ indicate the presence of small flux enhancements associated with solar fluxes at 0.6 - 13 MeV.

[Note: Counting rates for 29 - 30 August and 2 - 5 September may require corrections due to saturation of the instrument.]

Fig. 3 The proton counting rate in the energy range 0.6 - 13 MeV ($D_1 \bar{D}_2 \bar{D}_4$ coincidence) averaged over 30-minute intervals. Data points with error bars are derived from storage mode data from the spacecraft. Typical proton flux onsets described in this paper are observed on 25 December 1965 and 13 January 1966. Proton flux cut-offs appear on 4 January and 28 January 1966. The hourly counting rate of the Climax neutron monitor displays the modulation of galactic cosmic rays > 3 GV in magnetic rigidity arising from the presence of large-scale magnetic regions in space. Fan, Lamport, Simpson and Smith (1966) discuss the co-rotating event observed on 2 January 1966 by the Pioneer-6 and IMP-3 spacecraft.

Fig. 4 Thirty-minute averages of the counting rates of protons 13-70 MeV and 0.6 - 13 MeV. The enhanced flux of 0.6 - 13 MeV protons during 15-31 March is attributed to solar region 8207. The first evidence of enhanced flux from the following region (8223) appears on 31 March. A magnetic sector boundary (Ness, 1967) occurs on 31 March. Note at this time the abrupt change in the level of modulation at the Climax neutron monitor. (a) . . . (h) denote discrete flare and shock-wave events seen at 13 -70 MeV.

Fig. 5 Thirty-minute averages of 0.6 - 13 MeV protons. The onset of flux occurs late on 22 August. After the occurrence of large flares has increased the flux level, a cut-off is observed on 8 September. This cut-off was observed to co-rotate between the Pioneer-7 and IMP-3 spacecraft. The Climax neutron monitor shows an abrupt cessation of the Forbush decrease.

Fig. 6 Detailed plots of the low-energy flux onsets. 30-minute averages have been taken. The increases marked with asterisks on 4 and 5 July are probably of magnetospheric origin.

Fig. 7 Solar longitude of active centers during periods of enhanced low-energy proton flux. The rectangles extend from flux onset to flux cut-off. Longitude is measured with respect to the Sun-spacecraft line. The center is identified by the McMath plage number. (a) is the position of the birth of region 8105, and (b) indicates the position at which region 8362 begins to develop rapidly.

Fig. 8 Solar map showing the locations of plage regions 8207 and 8223 on the Sun (adapted from the Synoptic charts of the solar chromosphere, Meudon Observatory, France). Rotation numbers follow the international convention. Carrington coordinates (fixed on the solar disk) are used.

Fig. 9 Proton differential energy spectra from 3 periods of Pioneer-7 low-energy analysis mode (calibrate mode). (a) is a quiet period, when the $D_1\bar{D}_2\bar{D}_4$ counting rate was at or near background. (b) and (c) are two representative periods during the period of enhanced low-energy proton flux prior to the large proton event of 28 August 1966. Analysis was cut off below 0.8 MeV to avoid electron flux contributions.

Fig. 10 Directional distributions for protons 0.8 - 2 MeV during the three periods covered by Figure 9. In (b) and (c) an isotropic background similar to (b) has been subtracted. As in Figure 9, any possible electron contribution has been eliminated by cutting off the analysis below 0.8 MeV.

Fig. 11 A proposed model to illustrate the connection of the magnetic field from the active center to the interplanetary magnetic field. The dashed line concentric with the Sun indicates the height in the corona at which the magnetic field takes on its spiral form. For the flux onset on 15 March (Figure 4), events (b) and (f) and flux cut-off on 31 March, the position of the spacecraft is shown in a coordinate system in which the active center is stationary. Note: the dashed portion of the spiral field lines indicates a fore-shortening of the radial scale in this region.

Fig. 12 Proton differential energy spectrum during event (b) in Figure 4. This spectrum was observed during the period of maximum flux in the energy interval 13 - 70 MeV.

Fig. 13 Directional distribution of protons during the onset phases of events (b) and (e) in Figure 4, as shown in (a) and (b). An isotropic flux of galactic protons has been subtracted.

Fig. 14 Quadrant counting rates for the flare event of 24 March 1966. The orientation of the quadrants with respect to the Sun is shown in the inset. The increase in counting rate starting at 0230 U.T. (dashed portion of the quadrant 2 curve) is due to solar flare electrons. Protons first begin to arrive at ~ 0250 U.T.; after this time the relative contribution of electrons to the total intensity is small.

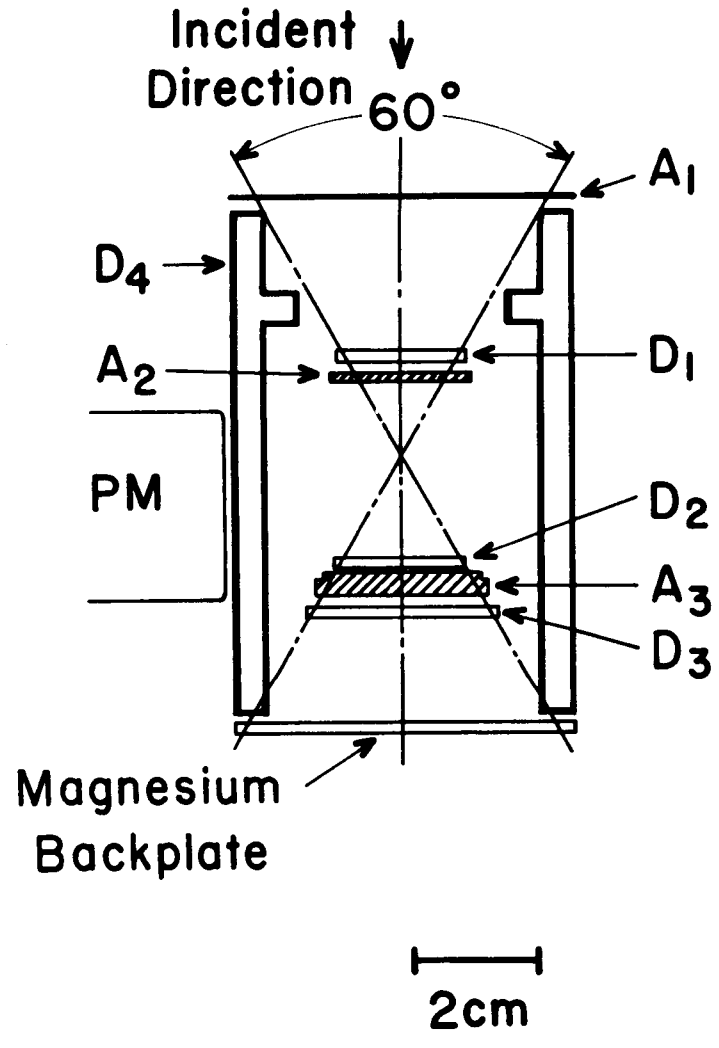

A_1 Aluminized Mylar Window

D_1 Lithium Drift Silicon Detector

A_2 Aluminum Absorber

D_2 Lithium Drift Silicon Detector

A_3 Platinum Absorber

D_3 Lithium Drift Silicon Detector

D_4 Plastic Scintillator

PM Photo Multiplier Tube

Pioneer-6/7 Cosmic Ray Telescope
The University of Chicago

Figure 1

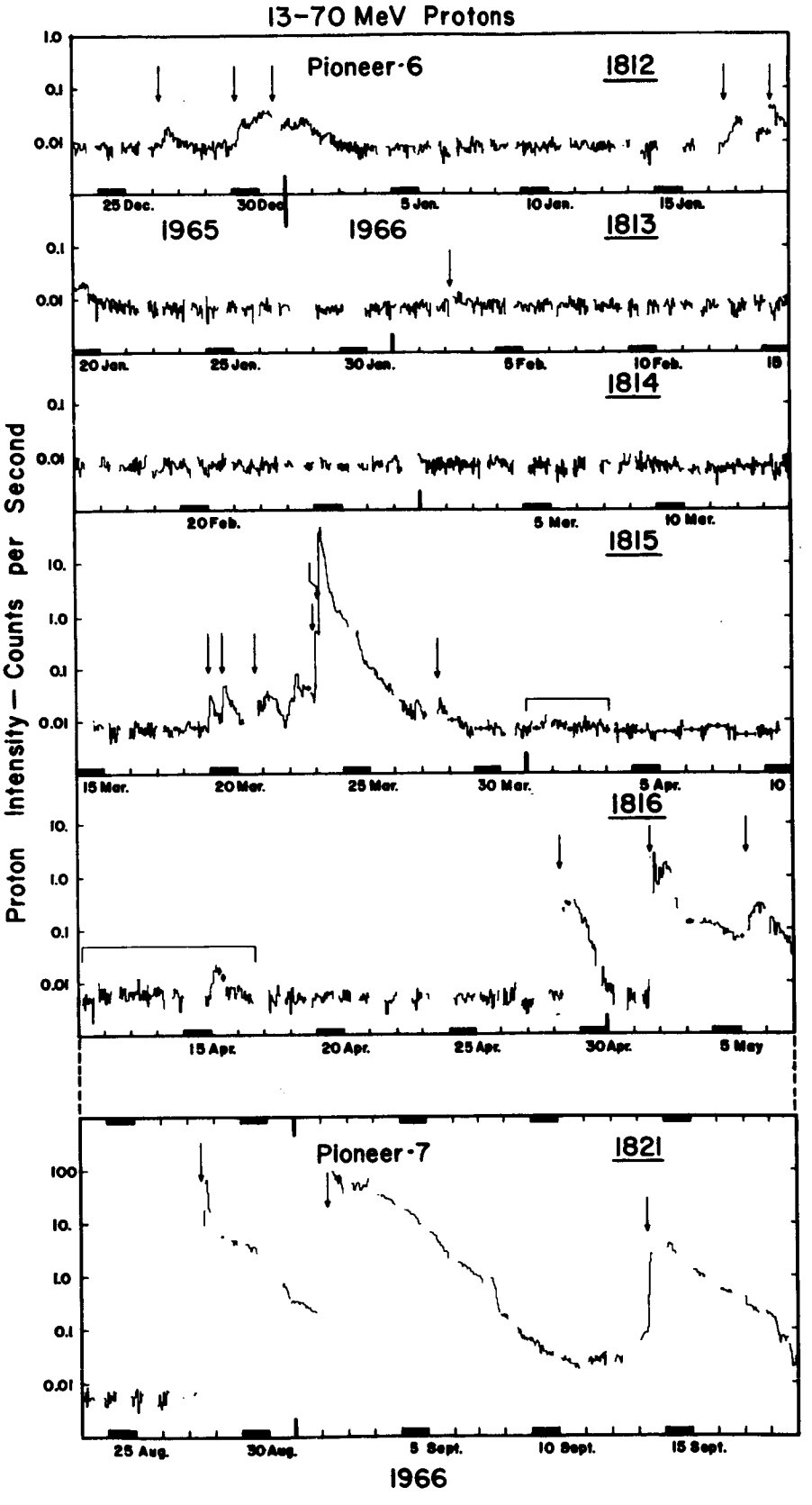
13-70 MeV Protons
Pioneer-6
1812
1965
1966
1813
1814
1815
1816
Pioneer-7
1821
Proton Intensity — Counts per Second
1.0
0.1
0.01
10.
1.0
0.1
0.01
100
10.
1.0
0.1
0.01
25 Dec.
30 Dec.
5 Jan.
10 Jan.
15 Jan.
20 Jan.
25 Jan.
30 Jan.
5 Feb.
10 Feb.
20 Feb.
5 Mar.
10 Mar.
15 Mar.
20 Mar.
25 Mar.
30 Mar.
5 Apr.
15 Apr.
20 Apr.
25 Apr.
30 Apr.
5 May
25 Aug.
30 Aug.
5 Sept.
10 Sept.
15 Sept.
1966

Figure 2

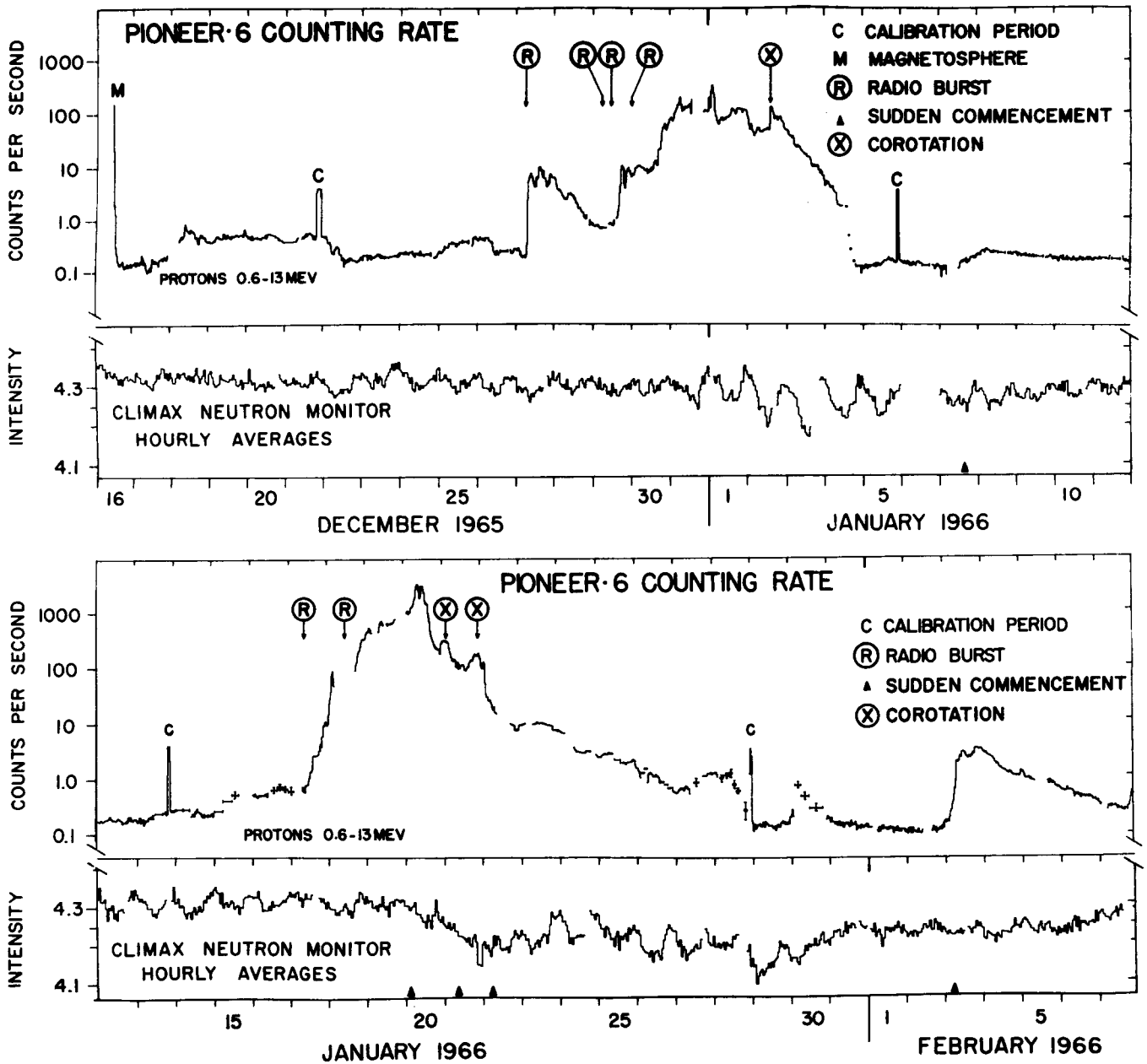
PIONEER·6 COUNTING RATE
C CALIBRATION PERIOD
M MAGNETOSPHERE
R RADIO BURST
SUDDEN COMMENCEMENT
X COROTATION
COUNTS PER SECOND
1000
100
10
1.0
0.1
PROTONS 0.6-13 MEV
INTENSITY
4.3
4.1
CLIMAX NEUTRON MONITOR
HOURLY AVERAGES
16
20
25
30
1
5
10
DECEMBER 1965
JANUARY 1966
PIONEER·6 COUNTING RATE
C CALIBRATION PERIOD
R RADIO BURST
SUDDEN COMMENCEMENT
X COROTATION
COUNTS PER SECOND
PROTONS 0.6-13 MEV
INTENSITY
CLIMAX NEUTRON MONITOR
HOURLY AVERAGES
15
20
25
30
1
5
JANUARY 1966
FEBRUARY 1966

Figure 3

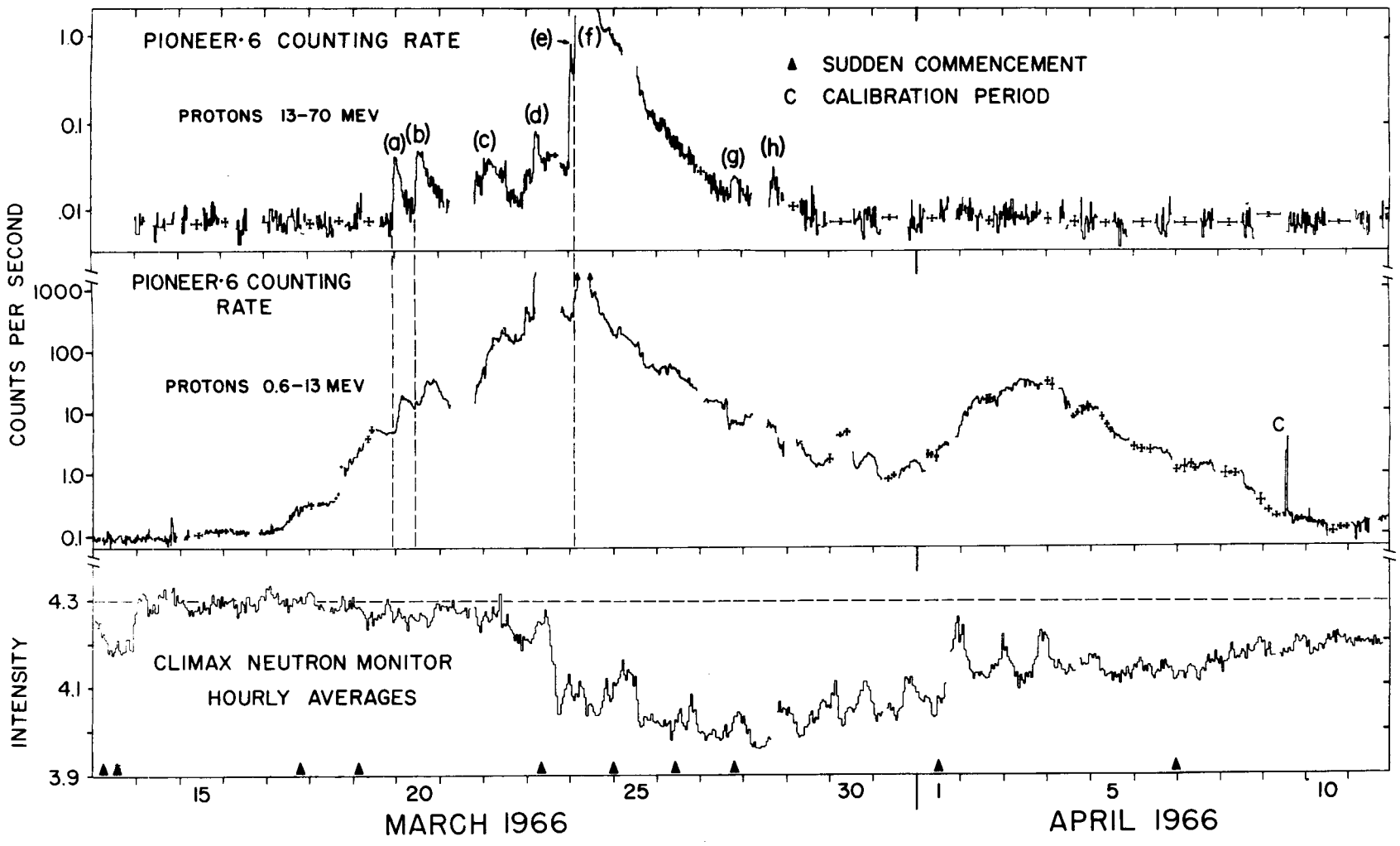
PIONEER·6 COUNTING RATE
PROTONS 13–70 MEV
(a)
(b)
(c)
(d)
(e)
(f)
(g)
(h)
▲ SUDDEN COMMENCEMENT
C CALIBRATION PERIOD
PIONEER·6 COUNTING RATE
PROTONS 0.6–13 MEV
C
COUNTS PER SECOND
1.0
0.1
.01
1000
100
10
1.0
0.1
CLIMAX NEUTRON MONITOR
HOURLY AVERAGES
INTENSITY
4.3
4.1
3.9
15
20
25
30
1
5
10
MARCH 1966
APRIL 1966

Figure 4

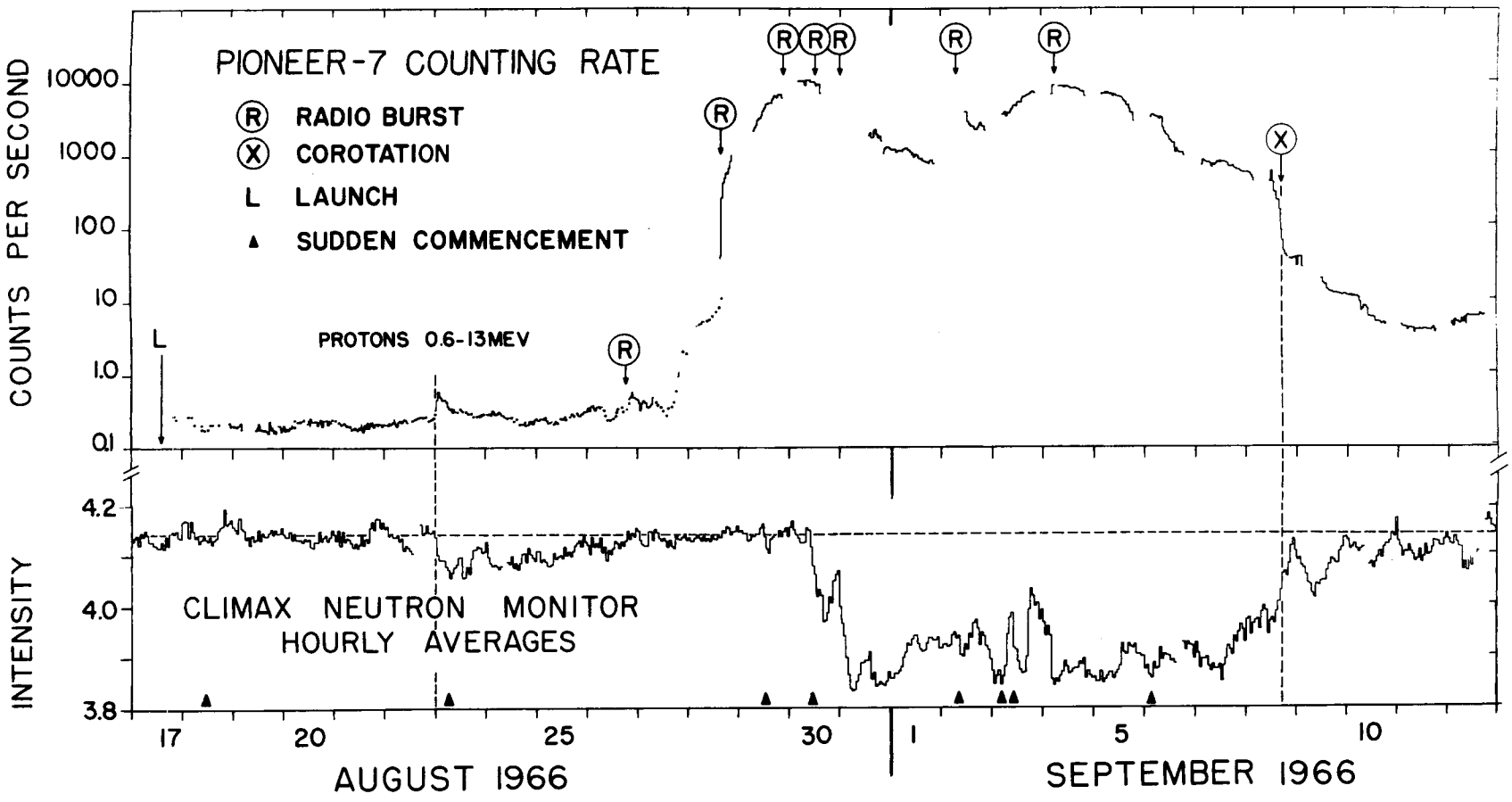
PIONEER-7 COUNTING RATE
R RADIO BURST
X COROTATION
L LAUNCH
▲ SUDDEN COMMENCEMENT
PROTONS 0.6-13MEV
COUNTS PER SECOND
10000
1000
100
10
1.0
0.1
INTENSITY
4.2
4.0
3.8
CLIMAX NEUTRON MONITOR
HOURLY AVERAGES
17
20
25
30
1
5
10
AUGUST 1966
SEPTEMBER 1966

Figure 5

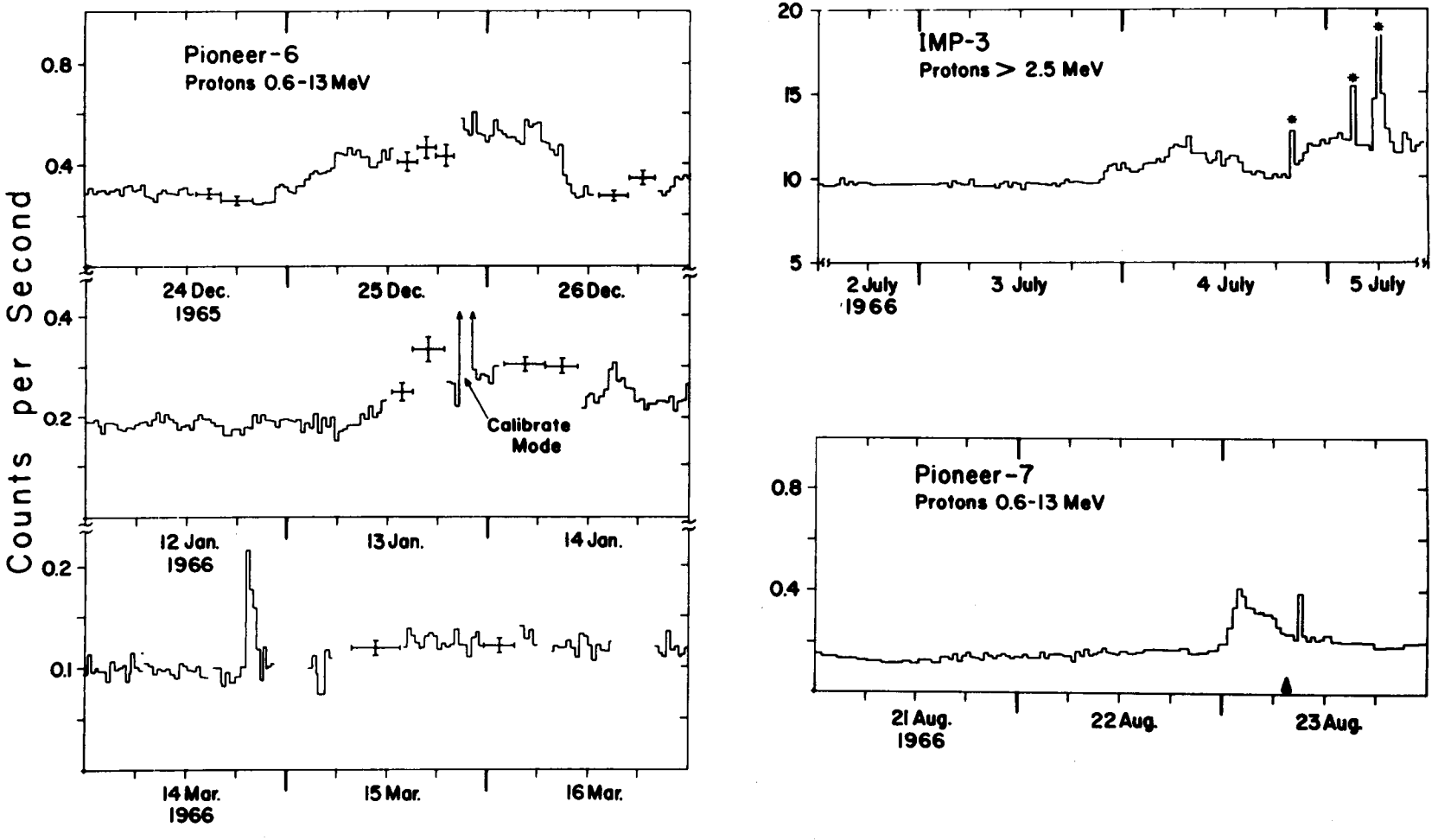
Pioneer-6
Protons 0.6-13 MeV
Counts per Second
0.8
0.4
24 Dec.
1965
25 Dec.
26 Dec.
0.4
0.2
Calibrate
Mode
12 Jan.
1966
13 Jan.
14 Jan.
0.2
0.1
14 Mar.
1966
15 Mar.
16 Mar.
IMP-3
Protons > 2.5 MeV
20
15
10
5
2 July
1966
3 July
4 July
5 July
Pioneer-7
Protons 0.6-13 MeV
0.8
0.4
21 Aug.
1966
22 Aug.
23 Aug.

Figure 6

Periods of Enhanced Fluxes of 0.6-13 MeV Protons

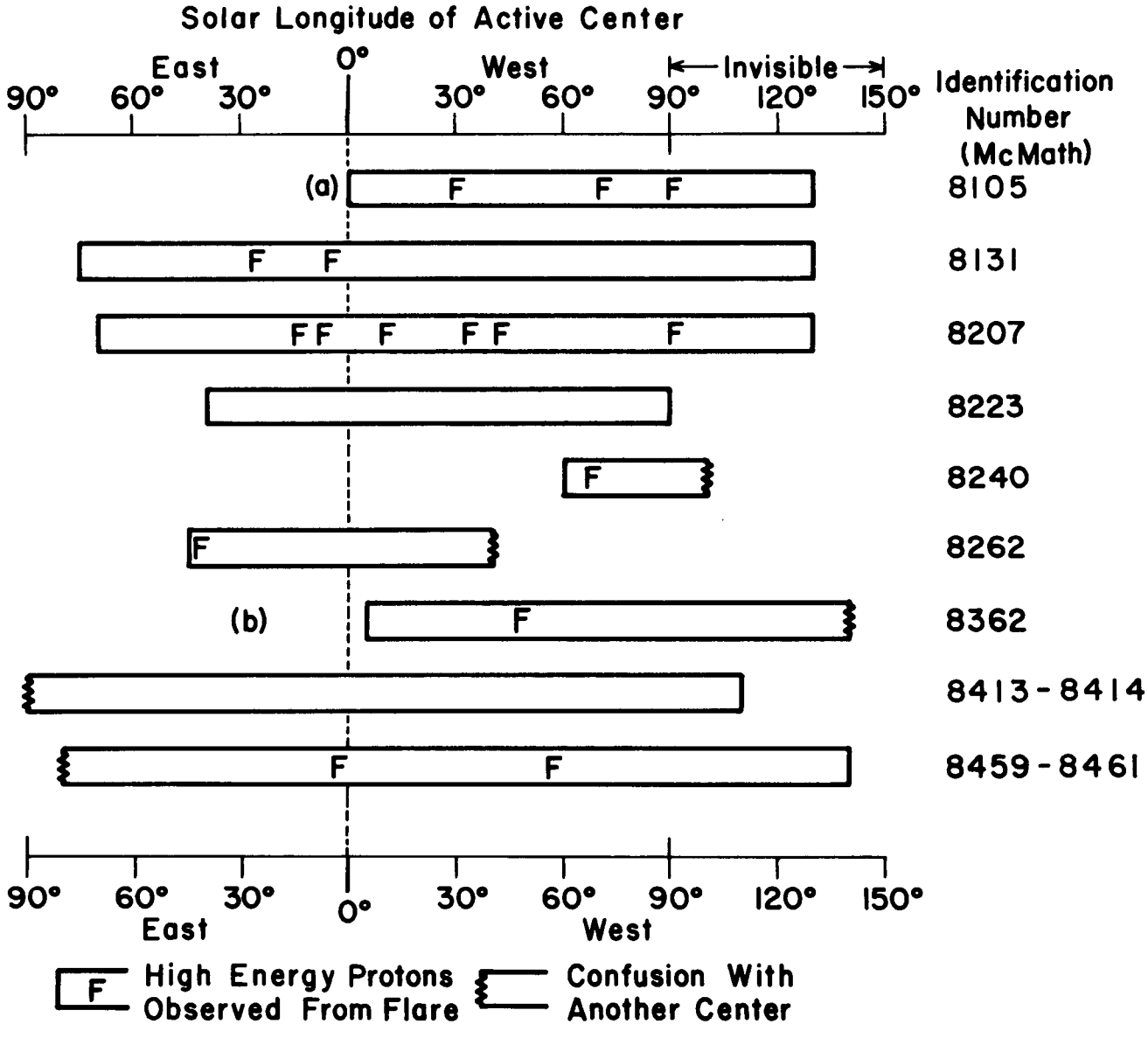

Figure 7

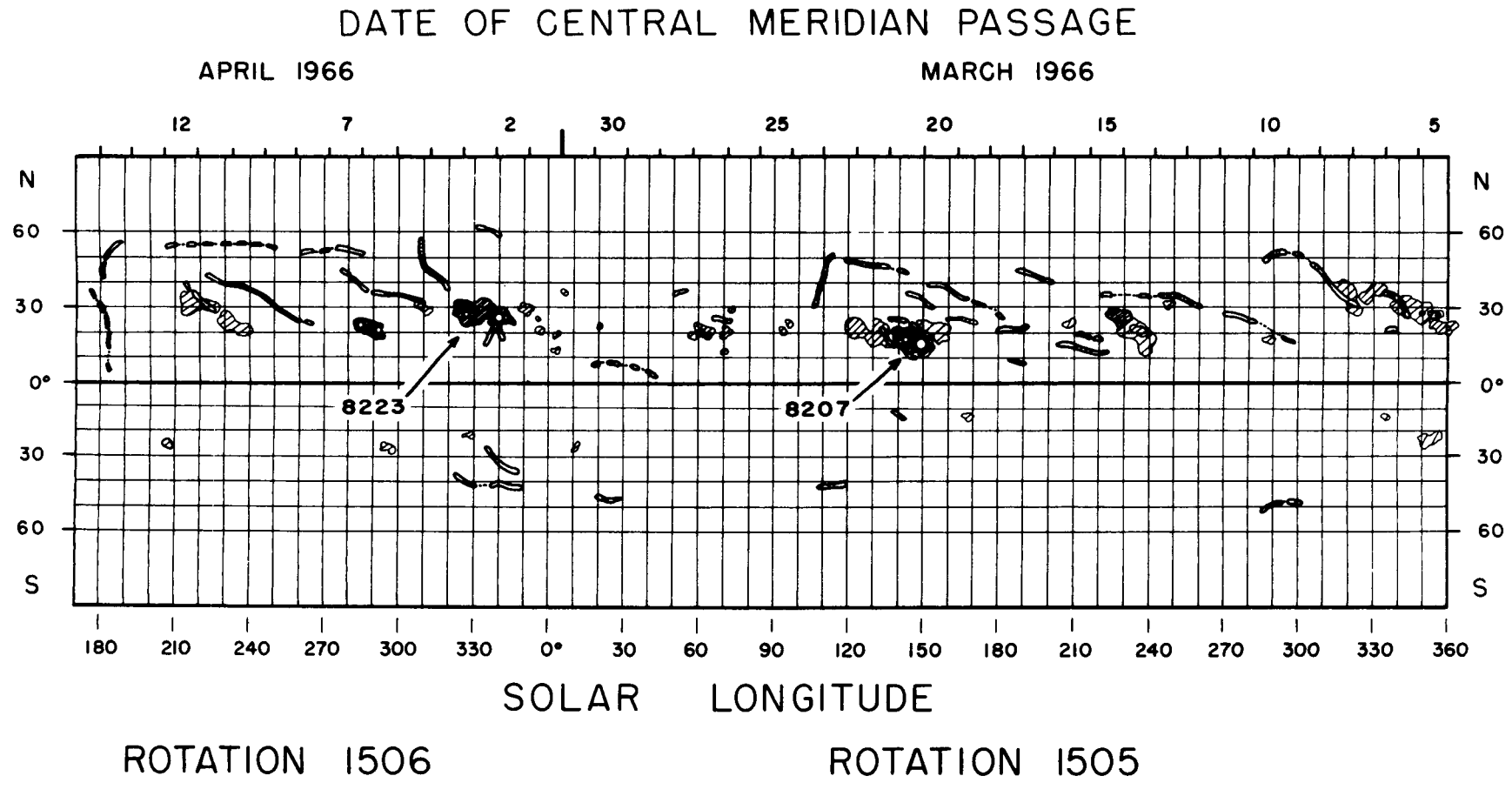
DATE OF CENTRAL MERIDIAN PASSAGE
APRIL 1966
MARCH 1966
12
7
2
30
25
20
15
10
5
N
60
30
0°
30
60
S
8223
8207
180
210
240
270
300
330
0°
30
60
90
120
150
180
210
240
270
300
330
360
SOLAR LONGITUDE
ROTATION 1506
ROTATION 1505

Figure 8

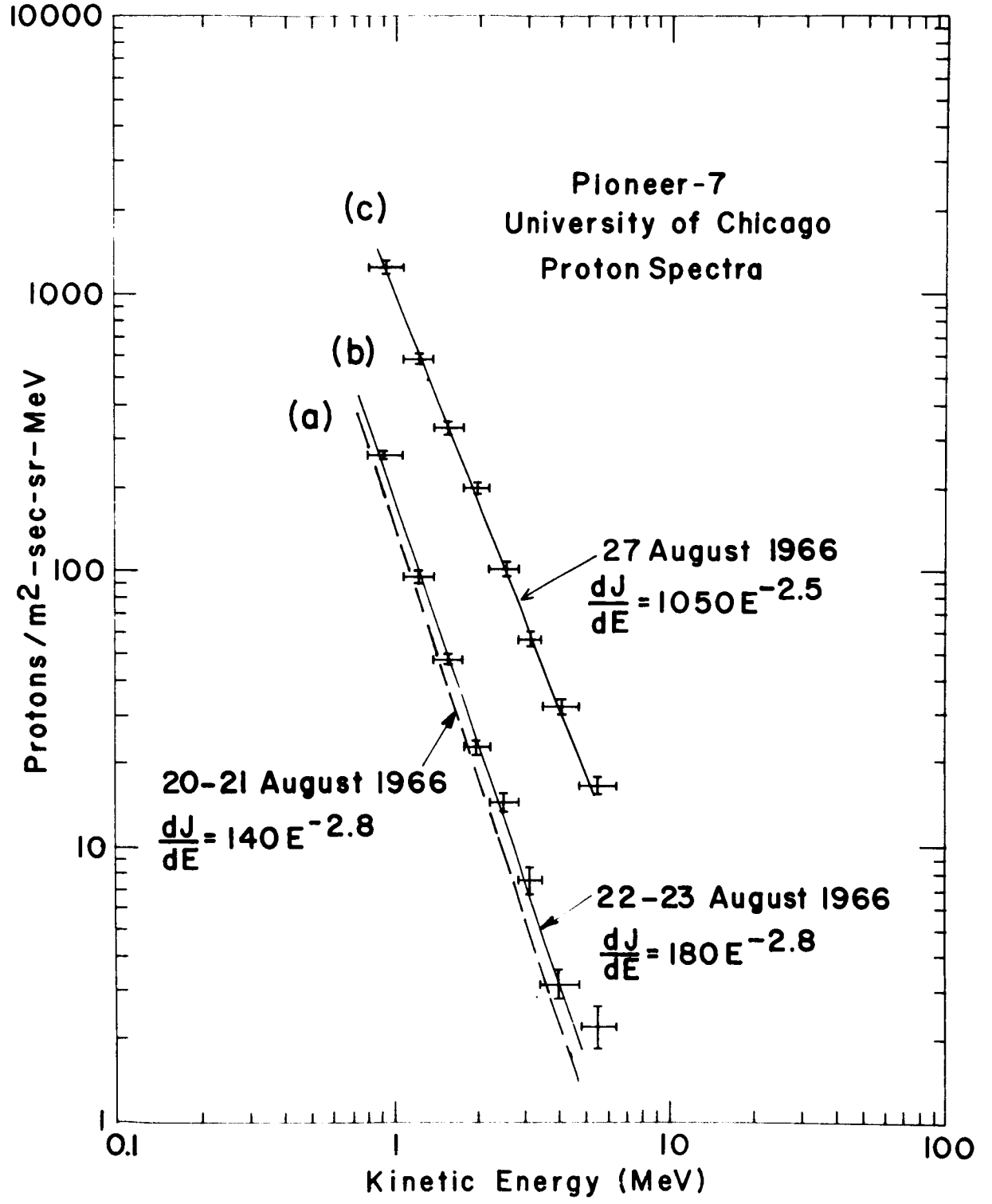
Pioneer-7
University of Chicago
Proton Spectra
(c)
(b)
(a)
27 August 1966
dJ/dE = 1050 E^-2.5
20-21 August 1966
dJ/dE = 140 E^-2.8
22-23 August 1966
dJ/dE = 180 E^-2.8
Protons / m2-sec-sr-MeV
Kinetic Energy (MeV)
10000
1000
100
10
1
0.1
1
10
100

Figure 9

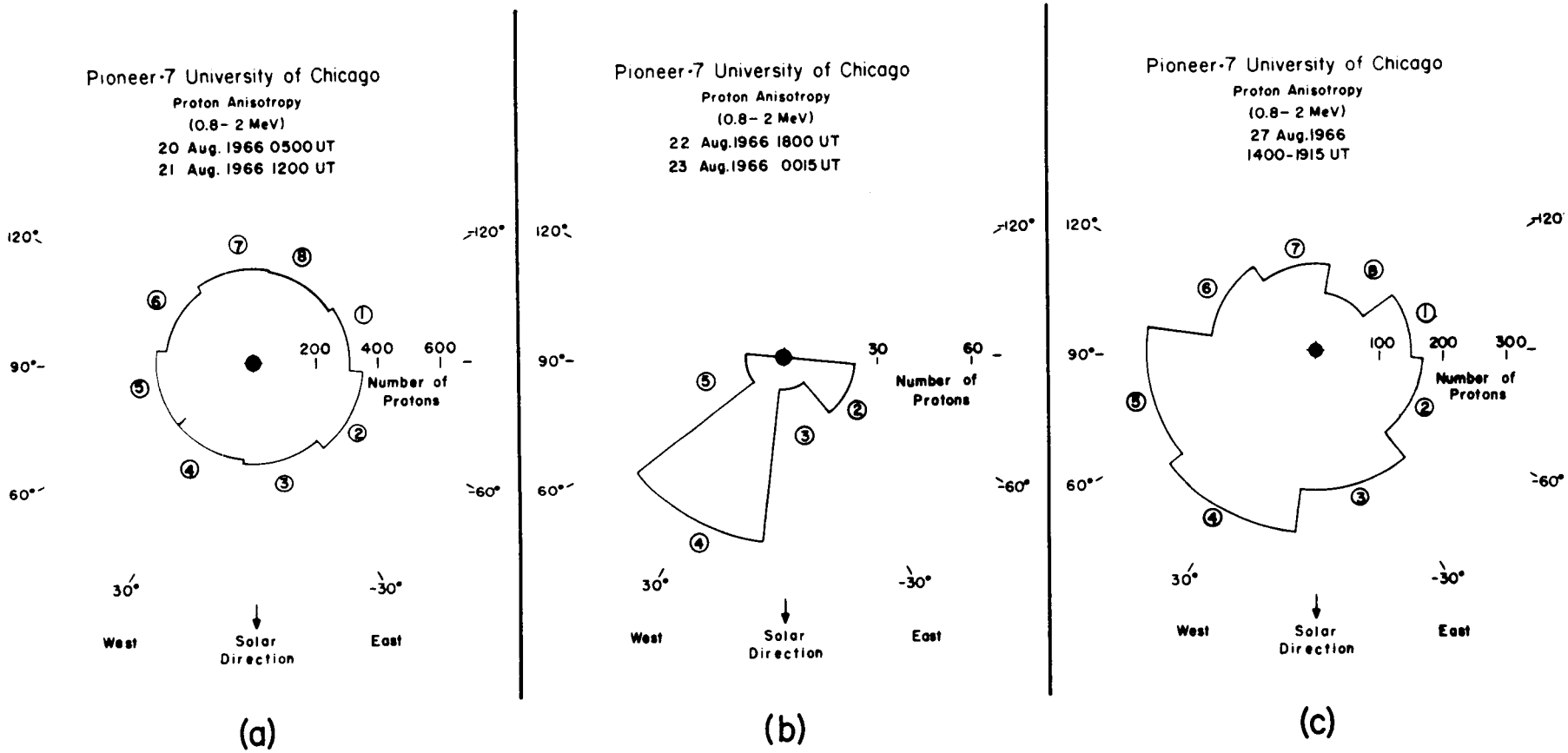
Pioneer-7 University of Chicago
Proton Anisotropy
(0.8- 2 MeV)
20 Aug. 1966 0500 UT
21 Aug. 1966 1200 UT
120°
90°
60°
200
400
600
Number of Protons
30°
-30°
West
Solar Direction
East
(a)
Pioneer-7 University of Chicago
Proton Anisotropy
(0.8- 2 MeV)
22 Aug.1966 1800 UT
23 Aug.1966 0015 UT
30
60
Number of Protons
(b)
Pioneer-7 University of Chicago
Proton Anisotropy
(0.8- 2 MeV)
27 Aug.1966
1400-1915 UT
100
200
300
Number of Protons
(c)

Figure 10

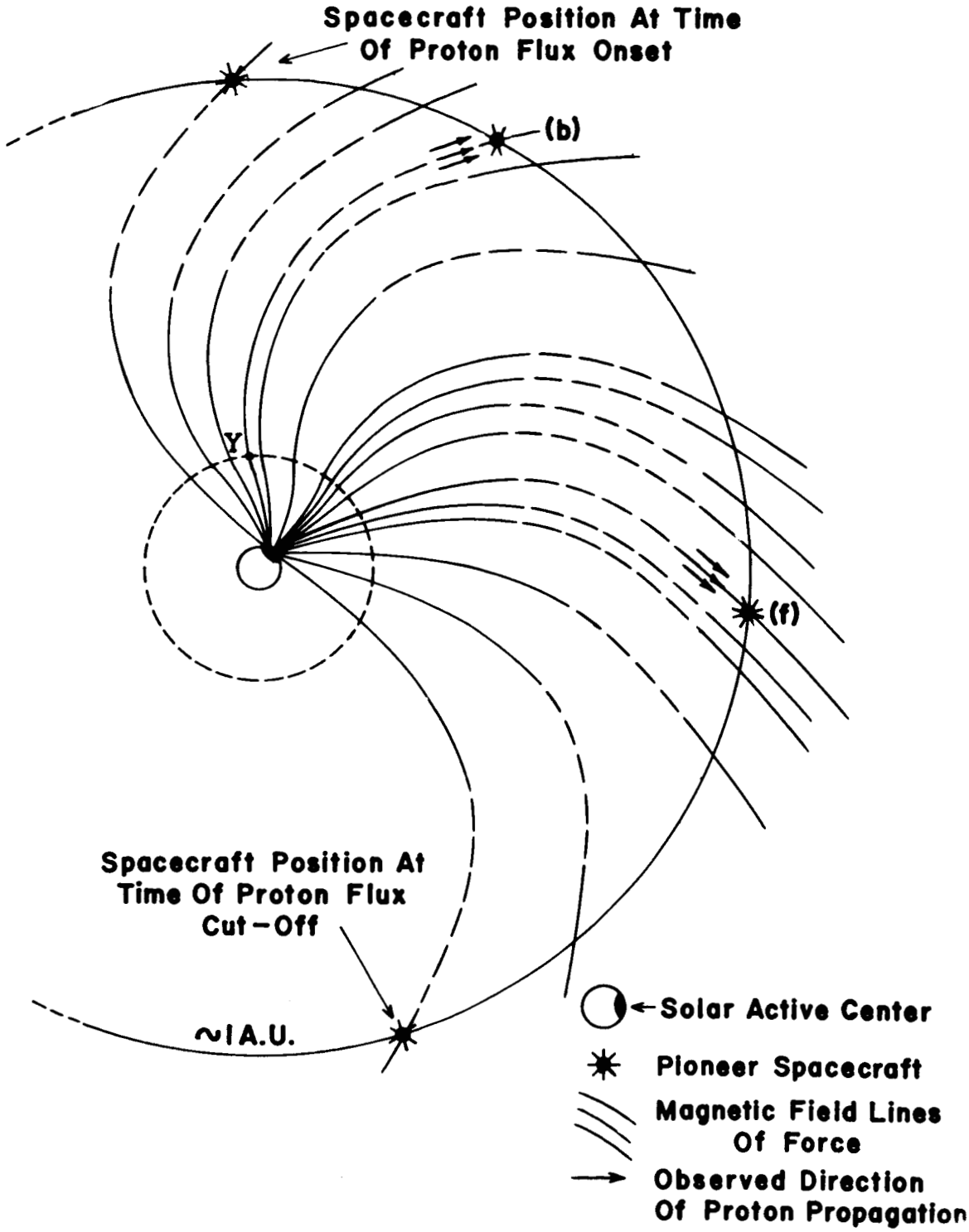
Spacecraft Position At Time
Of Proton Flux Onset
(b)
Y
(f)
Spacecraft Position At
Time Of Proton Flux
Cut-Off
~1A.U.
Solar Active Center
Pioneer Spacecraft
Magnetic Field Lines
Of Force
Observed Direction
Of Proton Propagation

Figure 11

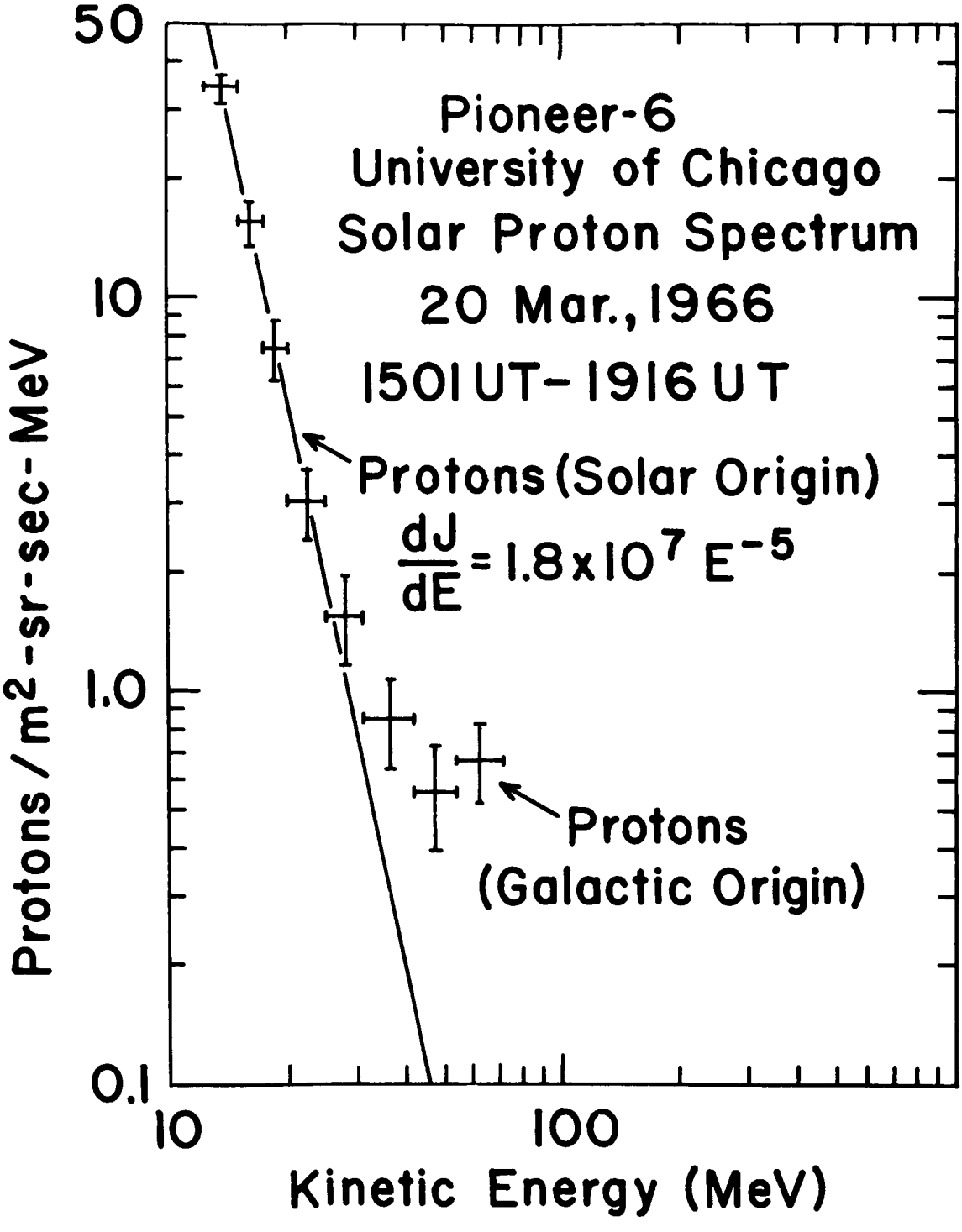
50
10
1.0
0.1
10
100
Protons / m2-sr-sec-MeV
Kinetic Energy (MeV)
Pioneer-6
University of Chicago
Solar Proton Spectrum
20 Mar., 1966
1501 UT - 1916 UT
Protons (Solar Origin)
dJ/dE = 1.8x10^7 E^-5
Protons
(Galactic Origin)

Figure 12

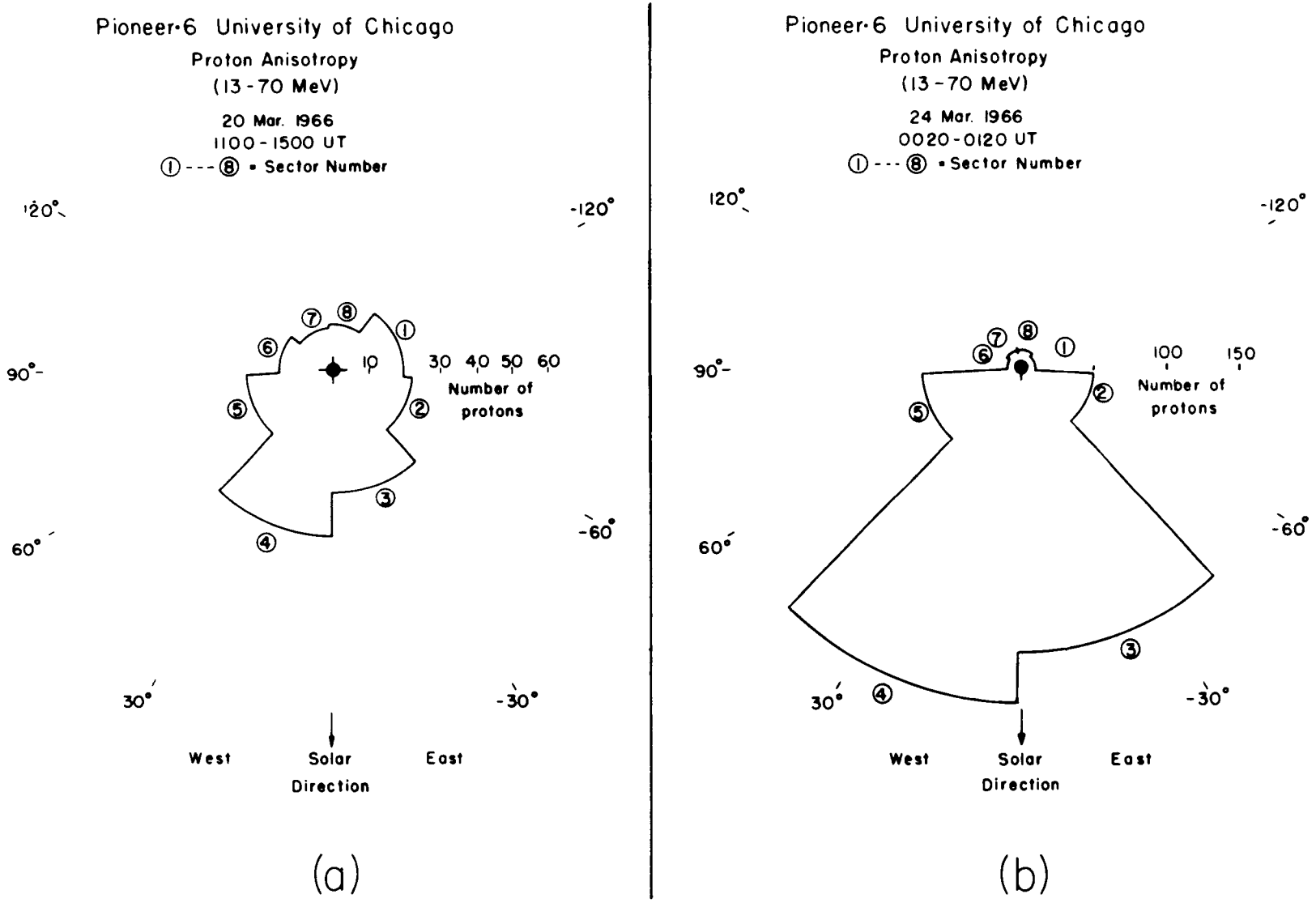
Pioneer-6 University of Chicago
Proton Anisotropy
(13-70 MeV)
20 Mar. 1966
1100-1500 UT
① --- ⑧ • Sector Number
120°
-120°
90°
60°
-60°
30°
-30°
10
30 40 50 60
Number of protons
West
Solar Direction
East
(a)
Pioneer-6 University of Chicago
Proton Anisotropy
(13-70 MeV)
24 Mar. 1966
0020-0120 UT
① --- ⑧ • Sector Number
120°
-120°
90°
60°
-60°
30°
-30°
100 150
Number of protons
West
Solar Direction
East
(b)

Figure 13

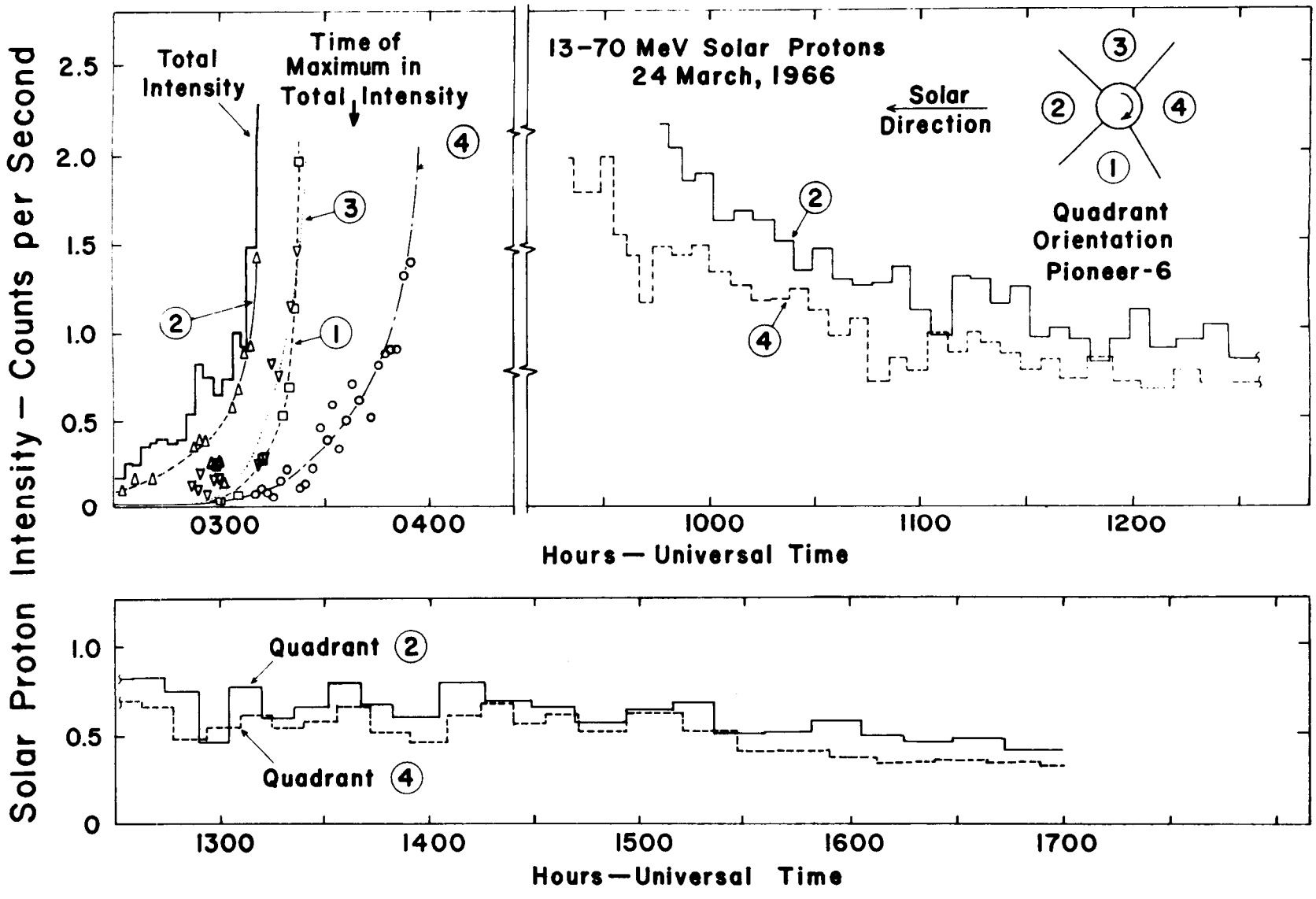
Solar Proton Intensity — Counts per Second
Total Intensity
Time of Maximum in Total Intensity
13–70 MeV Solar Protons
24 March, 1966
Solar Direction
Quadrant Orientation Pioneer-6
Hours — Universal Time
Quadrant (2)
Quadrant (4)
Hours — Universal Time

Figure 14